



MASTER THESIS

QUANTUM-ENHANCED ESTIMATION OF A MODE PARAMETER

PAU COLOMER SAUS

Supervisor: Dr. Manuel Gessner

July 2022

This master thesis describes analytical and numerical studies of quantum mode parameter estimation limits. We analyze the estimation of transverse displacements and wavelength variations using a parameter-independent quantum state in different light modes. We find and evaluate systems where we can achieve a quantum-enhanced sensitivity beyond the standard quantum limit. Moreover, we find the modes and states in which we have to prepare the light, as well as the measurements we have to perform in order to achieve the maximum possible sensitivity. We compare the maximal sensitivity that can be obtained on the estimation of a radial displacement with optimal states on different light modes.

0 Acknowledgements

I would like to thank Dr. Manuel Gessner, who has not only supervised this project but also been a great tutor and teacher. His willingness to give his time so generously has been very much appreciated. Also, I would like to express my very great appreciation to ICFO for giving me the opportunity to work on a department of such high standards as the Quantum Information Group led by Antonio Acín.

Contents

0 Acknowledgements

1 Introduction	1
1.1 Classical Parameter Estimation	1
1.2 Quantum Parameter Estimation	1
1.3 Modes of the electromagnetic field	2
1.4 Mode Parameter Estimation	2
2 Objectives	4
3 Results	4
3.1 Estimation of a radial displacement in a given direction α	4
3.1.1 Estimation of a radial displacement using Hermite-Gauss modes	4
3.1.2 Estimation of a radial displacement using Laguerre-Gauss modes	6
3.1.3 Analytical optimization of the sensitivity over all possible states	9
3.1.4 Quasi-optimal state for transverse displacements as a rotated NOON	11
3.1.5 Numerical optimization of transverse displacements	12
3.1.6 Application: Displacement on an arbitrary direction	14
3.2 Estimation of a change on the wavelength	16
3.2.1 We populate a single arbitrary Hermite mode	16
3.2.2 We populate a pair HG_{00} and $(HG_{02} + HG_{20})/\sqrt{2}$	16
3.2.3 Optimization of the sensitivity in wavelength variations	17
3.2.4 Numerical analysis of the quasi-optimal procedure in the estimation of a wavelength displacement	17
4 Conclusions	18
Bibliography	20
A Schwinger code	21
B Optimal state code	23
C Comparison code	25
D NOONs code	27
E Sensitivities for different angles	29
F Actual mode shape of the four strategies in figure 8	31
G Random state generation	34

1 Introduction

1.1 Classical Parameter Estimation

Consider a continuous random variable X that is modeled by a parameter depending density function. Picture a normal distribution, for example, it depends on two parameters: the mean $\mu = \mathbb{E}(X)$, and the variance $\sigma^2 = \text{var}(X) = \mathbb{E}[(X - \mu)^2]$. By measuring N times our variable, we will obtain a set of randomly distributed outcomes $[x_1, \dots, x_N]$. **Parameter estimation** aims to accurately determine the value of the parameters that determine the probability function from the set of outcomes.

We call an **estimator** a function of the set of results. For instance, the average of a set of observed variables is an estimator of the mean $\mu_{\text{est}}(x_1, \dots, x_N) = \sum_{i=1}^N x_i/N$, a parameter of the normal distribution. We say that an estimator is **unbiased** if its expected value coincides with the parameter we want to estimate. In the example before, this is $\mathbb{E}(\mu_{\text{est}}) = \mu$. We aim to find an unbiased estimator with the smallest possible **variance**.

The smallest variance that can be achieved in the estimation of a parameter θ , is given by the **Cramér-Rao bound** $\text{var}(\theta_{\text{est}}) \geq 1/I(\theta)$ [Rao92, Cra99]. Where $I(\theta)$ is the **Fisher information** (FI) [Fis22]. Given a parameter dependent distribution $f(x|\theta)$ that describes the probability to observe the event x given θ , the FI is the amount of information that X carries about θ , and it is defined as:

$$I(\theta) := \mathbb{E} \left[\frac{1}{f(x|\theta)^2} \left(\frac{\partial f(x|\theta)}{\partial \theta} \right)^2 \right]. \quad (1)$$

1.2 Quantum Parameter Estimation

In **quantum parameter estimation** the parameter is encoded in a quantum state $\hat{\rho}(\theta)$. In order to extract information about θ we have to perform measurements. According to the principles of quantum mechanics, the outcomes of the measurements are random variables with probability distributions given by the Born rule: $p(x|\theta) = \text{Tr}[\hat{\rho}(\theta)\hat{E}_x]$. Where $\{\hat{E}_x\}$ is a POVM (positive operator-valued measure), a set of semidefinite positive operators with the property $\sum_x \hat{E}_x = \mathbb{1}$ that characterize the measurement.

It is important to notice that, in the quantum world, the probability distribution depends on the choice of measurement. Quantum parameter estimation aims to find the measurement that will give us optimal data for our estimation. The **quantum Fisher information** (QFI) is defined as the optimization of the FI over all possible measurements $F_Q[\hat{\rho}(\theta)] := \max_{\{E_x\}} I(\theta)$. In other words, each measurement gives us a probability distribution through the Born rule, with these distributions we can calculate the Fisher information, the maximum of the FI (achieved with the optimal measurement) will be the quantum Fisher information.

The QFI can be expressed as $F_Q[\hat{\rho}(\theta)] = \text{Tr}[\hat{L}_\theta^2 \hat{\rho}(\theta)]$ [Hol11]. Where \hat{L}_θ is the **symmetric logarithmic derivative**, a self-adjoint operator that fulfills the equation:

$$\frac{\hat{L}_\theta \hat{\rho}(\theta) + \hat{\rho}(\theta) \hat{L}_\theta}{2} = \frac{\partial \hat{\rho}(\theta)}{\partial \theta}. \quad (2)$$

We can always find the optimal measurement by choosing the elements of our POVM to be the orthogonal projectors onto the eigenstates of \hat{L}_θ [BC94].

We can define a **quantum Cramér-Rao bound** [Hel69] in a very similar fashion as the classical one: $\text{var}(\theta_{\text{est}}) \geq 1/F_Q[\hat{\rho}(\theta)]$. If we measure N copies of a state to estimate a parameter θ , the QFI scales linearly with N , and we obtain $\text{var}(\hat{\theta}) \sim 1/N$. This scaling is

known as the **standard quantum limit** (SQL). However, we can improve the scaling of the measurement error beyond the SQL when using non-classical states [PS14, GLM11]. This quantum-enhanced behaviour can achieve an improvement of up to N on the error scaling $\text{var}(\hat{\theta}) \sim 1/N^2$, known as the **Heisenberg limit**.

1.3 Modes of the electromagnetic field

A mode of the electromagnetic field is a vector field $\mathbf{f}(\mathbf{r}, t)$ that is a normalized solution of the Maxwell equations in vacuum. $\forall t$ it fulfills the three equations:

$$\left(\Delta - \frac{1}{c^2} \frac{\partial^2}{\partial t^2}\right) \mathbf{f}(\mathbf{r}, t) = 0 \quad ; \quad \nabla \cdot \mathbf{f}(\mathbf{r}, t) = 0 \quad \text{and} \quad \frac{1}{V} \int_V d^3r |\mathbf{f}(\mathbf{r}, t)|^2 = 1. \quad (3)$$

With V the volume that contains the physical system. We can construct an **orthonormal mode basis** $\{\mathbf{f}_m(\mathbf{r}, t)\}$ on which we can decompose any solution of the equations in 3:

$$\frac{1}{V} \int_V d^3r \mathbf{f}_m^*(\mathbf{r}, t) \cdot \mathbf{f}_n(\mathbf{r}, t) = \delta_{m,n}. \quad (4)$$

We can therefore write any complex electromagnetic field as $\mathbf{E}^\dagger(\mathbf{r}, t) = \sum_m c_m \mathbf{f}_m(\mathbf{r}, t)$, where $\mathbf{E}(\mathbf{r}, t) = \mathbf{E}^\dagger(\mathbf{r}, t) + (\mathbf{E}^\dagger(\mathbf{r}, t))^*$. This implies that any given solution $\mathbf{E}(\mathbf{r}, t)$ of the Maxwell equations can be considered as a vector $\mathbf{c} = \{c_1, \dots, c_N\}$ belonging to a Hilbert space known as the **modal space**. In other words, any electromagnetic field can be expressed as a superposition of the elements of a mode basis. We always try to choose the most suitable mode basis for a given light source and optical system. Laguerre-Gauss modes, for example, are used in quantum key distribution [MMLO⁺15]; and temporal Hermite-Gauss modes provide a convenient orthogonal basis for light pulses [BRSR15].

Quantum light is described not only by its quantum state, but also by the electromagnetic field modes on which the state is defined [FT20]. For example, in order to completely describe the light coming out of a general laser, it is not enough to say "the light is in a coherent state". We also have to say "it is on the first element of the spatial Hermite-Gauss mode basis (which corresponds to a Gaussian beam shape)". In the same way that we can have light in a superposition of two quantum states, we can have light in a superposition of different modes. This latter superposition is described by the population of the elements in a chosen mode basis.

1.4 Mode Parameter Estimation

High-precision measurements in interferometry, spectroscopy, positioning and timing use light parameters to encode information. These parameters can be determined not only by the state of the light (such as the number of photons or the coherence), but also by the light-mode (such as the spatial profile or the frequency spectrum). There also exist properties that can be considered state or mode parameters such as the phase shift.

We have seen in section 1.2 that the sensitivity on the estimation of quantum parameters can surpass the SQL. The quantum limit on the estimation of an arbitrary mode parameter can be determined analytically [GTF22]. In fact, [GTF22] demonstrates that any mode parameter variation can be described as a change of the state given by an effective beam-splitter unitary evolution. The effective beam-splitter Hamiltonian depends on the shape of the modes:

$$\hat{H} = \sum_{jk} (f_j | f'_k) \hat{a}_j^\dagger \hat{a}_k, \quad (5)$$

where f'_k is the derivative of the k th mode with respect to the parameter θ we are estimating evaluated at $\theta = 0$, and $\hat{a}_i^{(\dagger)}$ are the creation and destruction operators of the mode labeled by the index i .

In the particular case when the parameter is imprinted by a unitary evolution generated by a Hamiltonian $\hat{\rho}(\theta) = \exp(-i\hat{H}\theta)\hat{\rho}\exp(i\hat{H}\theta)$, the quantum Fisher information is given by [BC94, TA14, PS14]:

$$F_Q[\hat{\rho}(\hat{\theta})]_{\theta=0} = F_Q[\hat{\rho}, \hat{H}] := 4\langle \hat{H}^2 \rangle_{\hat{\rho}} - 8 \sum_{n,m} \frac{p_n p_m}{p_n + p_m} |\langle \psi_n | \hat{H} | \psi_m \rangle|^2, \quad (6)$$

with $\hat{\rho}(\theta) = \sum_n p_n |\psi_n\rangle_\theta \langle \psi_n|_\theta$ the spectral decomposition of $\hat{\rho}(\theta)$. Notice $\hat{\rho} = \hat{\rho}(0)$ and $|\psi_n\rangle = |\psi_n\rangle_{\theta=0}$. By making a distinction between populated modes and the modes in the vacuum, [GTF22] derives the following expression for the quantum Fisher information:

$$F_Q[\hat{\rho}(\hat{\theta})]_{\theta=0} = F_Q[\hat{\rho}, \hat{H}_I] + 4 \sum_{kl \in I} \left[(f'_k | f'_l) - \sum_{j \in I} (f'_k | f_j)(f_j | f'_l) \right] \langle \hat{a}_k^\dagger \hat{a}_l \rangle_{\hat{\rho}}, \quad (7)$$

where I is the set of populated modes and

$$\hat{H}_I = i \sum_{jk \in I} (f_j | f'_k) \hat{a}_j^\dagger \hat{a}_k. \quad (8)$$

Notice that the first term in equation 7 can return quadratic values because of the element $\langle \hat{H}^2 \rangle$ in equation 6. This quadratic terms are the ones that can provide scaling beyond the SQL. This means that we can only achieve quantum enhancements beyond the SQL if $F_Q[\hat{\rho}, \hat{H}_I] \neq 0$. That is, if $H_I \neq 0$. Therefore, the origin of the high order terms that enable quadratic quantum scaling lays on the population of derivative modes such that $(f_j | f'_k) \neq 0$ for some $j, k \in I$.

In other words, if there is an overlap between the populated modes and their derivatives we may find quadratic scaling of the sensitivity on N . If the populated modes are orthogonal to their derivatives, the first term in equation 7 vanishes and the scaling will only be linear. Notice also that, if the derivatives of the populated modes can be written as linear combinations of the populated modes themselves, the second term (linear) in equation 7 will disappear.

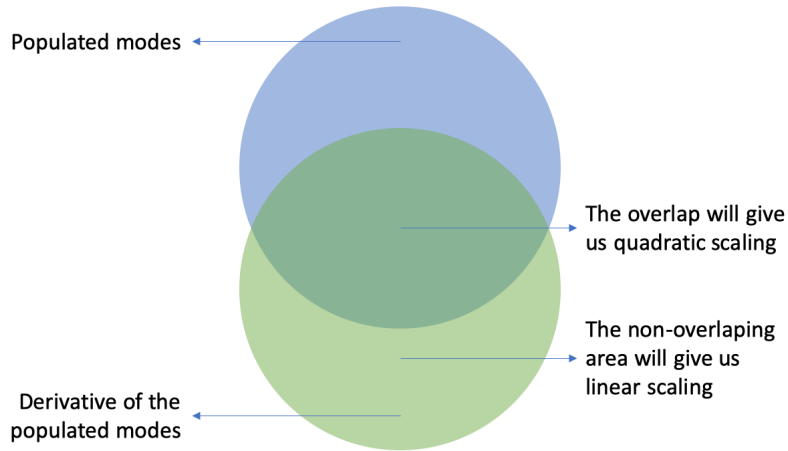


Figure 1: Visual representation of the relevant areas in the mode space

2 Objectives

The main objective of this project is to study the quantum enhancements that can be achieved in the estimation of a mode parameter. We know that this quantum enhancements can be achieved on the estimation of a displacement on the x and y axis using Hermite-Gauss modes (HG) [GTF22]. Therefore we expect to achieve similar enhancements on the estimation of a radial displacement on a given direction. We aim to generalize the results in the cited article and expand them by finding the state that achieves the maximal sensitivity on the estimation. We would also like to find the optimal measurement for this quantum estimation.

Laguerre-Gauss modes (LG) form another known and studied basis with a cylindrical symmetry. We want to analyze different mode schemes in this basis in order to see whether it is possible to achieve quantum enhancements beyond the SQL on the estimation of the same parameter as the case before, a radial displacement on a given direction. We also aim here to find the optimal state that maximizes the sensitivity and the optimal measurement.

If we achieve the previous objectives we would like to compare the characteristics of the HG and LG modes on the estimation of a radial displacement.

Furthermore, we will explore possibilities to achieve quantum enhancements in the estimation of other mode parameters such as the wavelength.

3 Results

3.1 Estimation of a radial displacement in a given direction α

We analyze the sensitivity that can be achieved in the estimation of a radial displacement in an arbitrary direction α . We study and compare different mode population schemes in two mode bases the *Hermite-Gauss modes* in section 3.1.1 and the *Laguerre-Gauss modes* in 3.1.2. In section 3.1.3 we focus on a two-mode scenario that allows us to study the estimation for a general case. We will find analytically a quasi-optimal state that achieves quasi-maximal sensitivity on the estimation. In section 3.1.4 we provide an interpretation for this quasi-optimal state through the Schwinger representation. We work numerically in 3.1.5 to find the actual optimal state, we compare it to our quasi-optimal analytical one, and interpret it using again the Schwinger representation. Finally, in section 3.1.6 we apply the obtained knowledge to discern which mode basis can achieve better sensitivities on the estimation of a radial displacement in a known and an unknown direction.

3.1.1 Estimation of a radial displacement using Hermite-Gauss modes

Hermite-Gauss modes are described by two indices n and m that determine the shape of the beam in the x and y direction respectively. They have a rectangular symmetry along the propagation z -axis (see figure 2), so we analyze them in Cartesian coordinates. Notice that the first mode HG_{00} is a regular Gaussian beam.

The mathematical expression for an arbitrary Hermite-Gauss mode reads:

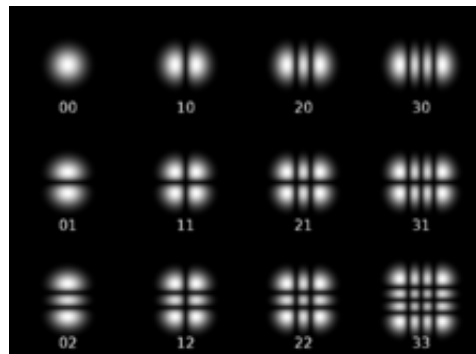


Figure 2: 12 Hermite-Gauss modes [CFB+13]

$$\begin{aligned}
HG_{nm}(x, y; z, w_0, k) &= \sqrt{\frac{2}{\pi 2^{n+m} n! m!}} \frac{1}{w(z)} H_n \left(\frac{\sqrt{2}x}{w(z)} \right) H_m \left(\frac{\sqrt{2}y}{w(z)} \right) \times \\
&\exp \left[-\frac{x^2 + y^2}{w(z)^2} \right] \exp \left[-ikz \frac{x^2 + y^2}{2(z^2 + z_R^2)} \right] \exp [i(n + m + 1)\psi(z)] \exp(-ikz),
\end{aligned} \tag{9}$$

where $H_k(x) = (-1)^k e^{x^2} \frac{d^k}{dx^k} e^{-x^2}$ is the k th Hermite polynomial, $w(z) = w_0 \sqrt{1 + (z/z_R)^2}$ is the beam radius and w_0 the beam waist. The Gouy phase is $\psi(z) = \arctan(z/z_R)$. The wave number k depends on the wavelength λ as $k = 2\pi/\lambda$, and $z_R = \pi w_0^2/\lambda$.

Our aim is to achieve quantum enhancements in the estimation of a radial displacement on an arbitrary direction α . This displacement produces a change on the Cartesian coordinates $x \rightarrow \tilde{x} = x + \delta r \cos \alpha$, and $y \rightarrow \tilde{y} = y + \delta r \sin \alpha$. As we saw in section 1.4, we may achieve enhancements over the SQL if there is an overlap between the populated modes and their derivatives. Let us start by finding a general expression for the derivative with respect to δr evaluated at $\delta r = 0$. By using the chain rule, the basic properties of the Hermite polynomials:

$$H_{n+1}(x) = 2xH_n(x) - \partial H_n(x) \quad \text{and} \quad \partial H_n(x) = 2nH_{n-1}(x), \tag{10}$$

and algebraic manipulations, we can identify the derivative as:

$$\begin{aligned}
\left. \frac{\partial HG_{nm}(\tilde{x}, \tilde{y})}{\partial \delta r} \right|_{\delta r=0} &= \frac{\cos \alpha}{w_0} \left[\sqrt{n} HG_{n-1, m} - \sqrt{n+1} HG_{n+1, m} \right] + \\
&\frac{\sin \alpha}{w_0} \left[\sqrt{m} HG_{n, m-1} - \sqrt{m+1} HG_{n, m+1} \right].
\end{aligned} \tag{11}$$

This simplifies the following calculations as the inner products that are required to determine the effective beam splitter Hamiltonian \hat{H}_I (equation 8) and the sensitivity F_Q (equation 7) can be solved trivially using the orthonormality condition of the mode basis $(HG_{nm}|HG_{pq}) = \delta_{np}\delta_{mq}$, instead of having to solve two-dimensional integrals. Let us calculate now the effective Hamiltonian and the sensitivity limit for different strategies based on HG modes.

a) *We populate a single mode HG_{nm}*

As we can see from equation 11, there is no overlap between HG_{nm} and its derivative. Therefore, if all modes besides HG_{nm} are in the vacuum, the effective Hamiltonian vanishes. This implies that we will not be able to achieve quadratic scaling on the sensitivity:

$$F_Q[\hat{\rho}(\delta r)]_{\delta r=0} = \left[\frac{4(2n+1)}{w_0^2} \cos(\alpha)^2 + \frac{4(2m+1)}{w_0^2} \sin(\alpha)^2 \right] \langle \hat{N}_{nm} \rangle_{\hat{\rho}}, \tag{12}$$

with $\hat{N}_{nm} = \hat{a}_{nm}^\dagger \hat{a}_{nm}$ the number operator for the photons in the mode HG_{nm} .

We can not obtain quantum enhancements beyond the standard quantum limit on the estimation of a radial displacement by populating a single HG_{nm} mode.

b) *We populate all modes from HG_{00} up to a HG_{nm}*

The derivative of HG_{nm} (equation 11) has non-vanishing overlap with its contiguous modes. In order to take full advantage of the effective Hamiltonian, we populate all modes up to a maximum HG_{nm} . Notice that the larger the effective Hamiltonian \hat{H}_I , the greater the quadratic terms will be and larger the quantum enhanced sensitivity. In this case the effective Hamiltonian reads:

$$\hat{H}_I = \frac{i}{w_0} \left[\cos \alpha \sum_{j=0}^m \sum_{k=0}^{n-1} \sqrt{k+1} (\hat{a}_{k,j}^\dagger \hat{a}_{k+1,j} - \hat{a}_{k+1,j}^\dagger \hat{a}_{k,j}) + \sin \alpha \sum_{k=0}^n \sum_{j=0}^{m-1} \sqrt{j+1} (\hat{a}_{k,j}^\dagger \hat{a}_{k,j+1} - \hat{a}_{k,j+1}^\dagger \hat{a}_{k,j}) \right]. \quad (13)$$

And the sensitivity:

$$F_Q[\hat{\rho}(\delta r)] = F_Q[\hat{H}_I, \hat{\rho}] + \frac{4(n+1)}{w_0^2} \cos(\alpha)^2 \sum_{j=0}^m \langle \hat{N}_{n,j} \rangle_{\hat{\rho}} + \frac{4(m+1)}{w_0^2} \sin(\alpha)^2 \sum_{k=0}^n \langle \hat{N}_{k,m} \rangle_{\hat{\rho}}. \quad (14)$$

The first term will provide quadratic scaling (remember equation 6). The linear scaling of the other terms is due to losses to the vacuum from the modes HG_{nj} and HG_{km} , $\forall k, j \in I$. Notice that the derivatives of these involve $HG_{n+1,j}$ and $HG_{k,m+1}$ which are not populated.

We can obtain quantum enhancements beyond the standard quantum limit in the estimation of radial displacements by populating contiguous HG modes.

The results in this section generalize the ones calculated [GTF22] for a displacement on the x or y -axis, which can be recovered as the special cases with $\alpha = 0$ and $\alpha = \pi/2$ respectively. A relevant unanswered question would be which is the state $\hat{\rho}$ that maximizes the sensitivity in this scenario. We will come back to this in section 3.1.3.

3.1.2 Estimation of a radial displacement using Laguerre-Gauss modes

Laguerre-Gauss modes exhibit a cylindrical symmetry described by the generalized Laguerre polynomials (see figure 3), $p \geq 0$ is the radial index and $m \in [-p, p]$ the azimuthal index. They are expressed in polar coordinates, and carry an intrinsic angular momentum along the propagation z -axis. Notice that the first mode LG_{00} is again a regular Gaussian beam.

The mathematical expression for an arbitrary Hermite-Gauss mode reads:

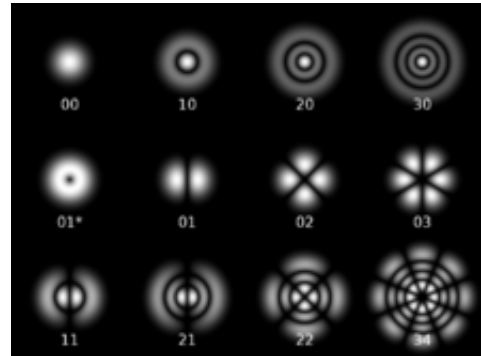


Figure 3: 12 Laguerre-Gauss modes [CFB+13]

$$LG_p^m(r, \theta, z) = \sqrt{\frac{2p!}{\pi(p+|m|)!}} \frac{1}{w(z)} \left(\frac{r\sqrt{2}}{w(z)} \right)^{|m|} L_p^{|m|} \left(\frac{2r^2}{w(z)^2} \right) \times \exp \left[\frac{-r^2}{w(z)^2} - \frac{ikr^2 z}{2(z^2 - z_R^2)} \right] \exp [i(2p + |m| + 1)\psi(z)] \exp(im\theta) \exp(-ikz). \quad (15)$$

With $L_p^m(x) = \sum_{i=0}^p (-1)^i \binom{p+m}{p-i} \frac{x^i}{i!}$ the generalized Laguerre polynomials. All the other terms in this equation have already been defined in section 3.1.1. If we perform a radial displacement δr in a given direction α , the variables in the Laguerre modes change as:

$$\begin{aligned} r = \sqrt{x^2 + y^2} &\longrightarrow \tilde{r} = \sqrt{(x + \delta r \cos(\alpha))^2 + (y + \delta r \sin(\alpha))^2} \\ \theta = \arctan\left(\frac{y}{x}\right) &\longrightarrow \tilde{\theta} = \arctan\left(\frac{y + \delta r \sin(\alpha)}{x + \delta r \cos(\alpha)}\right). \end{aligned} \quad (16)$$

Just as before, we start by calculating the derivative with respect to δr :

$$\begin{aligned} \left. \frac{\partial LG_p^m}{\partial \delta r} \right|_{\delta r=0} &= \frac{\sin(\alpha - \theta)}{r} im LG_p^m + \frac{\cos(\alpha - \theta)}{r} |m| LG_p^m - \\ &- \cos(\alpha - \theta) \frac{e^{-i\theta}}{w_0} \left(\sqrt{2p} LG_{p-1}^{m+1} + \sqrt{2(p + |m| + 1)} LG_p^{m+1} \right). \end{aligned} \quad (17)$$

To obtain this result we have used basic trigonometry relations and the recurrence properties of the generalized Laguerre polynomials: $L_n^{(m)}(x) = L_n^{(m+1)}(x) - L_{n-1}^{(m+1)}(x)$ and $nL_n^{(m)}(x) = (n+m)L_{n-1}^{(m)}(x) - xL_{n-1}^{(m+1)}(x)$. Notice that in this Laguerre-Gauss case we are not able to write the derivative of an arbitrary state as a function of other modes in the basis with coefficients that are independent of the coordinates r and θ . This forbids us to use the orthonormality relations to calculate inner product between modes. We are forced to perform double integrals over r and θ .

a) *We populate a single mode LG_{nm}*

The effective Hamiltonian $\hat{H}_I = i(LG_p^m | \partial LG_p^m \rangle \hat{a}_{pm}^\dagger \hat{a}_{pm}$ where ∂LG_p^m is:

$$\begin{aligned} \hat{H}_I &= \left[-m \left(LG_p^m \left| \frac{\sin(\alpha - \theta)}{r} LG_p^m \right. \right) - i \frac{\sqrt{2(p + |m| + 1)}}{w_0} \left(LG_p^m \left| \cos(\alpha - \theta) e^{-i\theta} LG_{p-1}^{m+1} \right. \right) + \right. \\ &+ \left. \frac{w(z)}{\sqrt{2}} i|m| \left(LG_p^m \left| \frac{\cos(\alpha - \theta)}{r} LG_p^m \right. \right) - i \frac{\sqrt{2p}}{w_0} \left(LG_p^m \left| \cos(\alpha - \theta) e^{-i\theta} LG_{p-1}^{m+1} \right. \right) \right] \hat{a}_{nm}^\dagger \hat{a}_{nm}. \end{aligned} \quad (18)$$

Notice that now the creation and annihilation $\hat{a}_{pm}^{(\dagger)}$ operators refer now to the LG_p^m mode. Lets focus on the angular parts of the inner product integrals:

$$\begin{aligned} \text{1st: } &\int_0^{2\pi} e^{-im\theta} \sin(\alpha - \theta) e^{im\theta} d\theta = 0 \\ \text{2nd=4th: } &\int_0^{2\pi} e^{-im\theta} \cos(\alpha - \theta) e^{i(m+1)\theta} e^{-i\theta} d\theta = 0 \\ \text{3rd: } &\int_0^{2\pi} e^{-im\theta} \cos(\alpha - \theta) e^{im\theta} d\theta = 0 \end{aligned} \quad (19)$$

The radial integrals converge, therefore the Hamiltonian is $\hat{H}_I = 0$.

We can not achieve quantum enhancements beyond the standard quantum limit on the estimation of a radial displacement by populating a single LG_n^m mode.

b) *We populate a pair LG_0^0 and LG_0^1*

The general expression for the effective Hamiltonian reads $\hat{H}_I = i \sum_{j,k \in \mathcal{I}} (f_j | f'_k) \hat{a}_j^\dagger \hat{a}_k$. We have already seen that the inner products $(LG_0^0 | \partial LG_0^0) = (LG_0^1 | \partial LG_0^1) = 0$ because the integral of the angular part is null. However, we still have to calculate $(LG_0^1 | \partial LG_0^0)$ and $(LG_0^0 | \partial LG_0^1)$. We have:

$$\begin{aligned} \left. \frac{\partial LG_0^0}{\partial \delta_r} \right|_{\delta_r=0} &= -\cos(\alpha - \theta) \frac{e^{-i\theta} \sqrt{2}}{w_0} LG_0^1 \\ \left. \frac{\partial LG_0^1}{\partial \delta_r} \right|_{\delta_r=0} &= i \frac{\sin(\alpha - \theta)}{r} LG_0^1 + \frac{\cos(\alpha - \theta)}{r} LG_0^1 - \cos(\alpha - \theta) \frac{2e^{-i\theta}}{w_0} LG_0^2. \end{aligned} \quad (20)$$

Then the inner products can be calculated by performing the double integrals. The first one results in:

$$(LG_0^1 | \partial LG_0^0) = -\frac{\sqrt{2}}{w_0} \int_0^{2\pi} \cos(\alpha - \theta) e^{-i\theta} d\theta \int_0^\infty r dr \frac{4r^2}{\pi w(z)^4} e^{-\frac{2r^2}{w(z)^2}} = -\frac{e^{-i\alpha}}{\sqrt{2}w_0} \quad (21)$$

We know that the hermicity condition $(f'_k | f_j) + (f_k | f'_j) = 0, \forall k, j \in \mathcal{I}$ has to be fulfilled. Then we expect $(LG_0^0 | \partial LG_0^1) = e^{i\alpha} / \sqrt{2}w_0$. Lets check it explicitly:

$$\begin{aligned} (LG_0^0 | \partial LG_0^1) &= i \int_0^{2\pi} \sin(\alpha - \theta) e^{i\theta} d\theta \int_0^\infty r dr \frac{2\sqrt{2}}{\pi w(z)^3} e^{-\frac{2r^2}{w(z)^2}} e^{i\psi} + \\ &+ \int_0^{2\pi} \cos(\alpha - \theta) e^{i\theta} d\theta \int_0^\infty r dr \frac{2\sqrt{2}}{\pi w(z)^3} e^{-\frac{2r^2}{w(z)^2}} e^{i\psi} - \\ &- \frac{2}{w_0} \int_0^{2\pi} \cos(\alpha - \theta) e^{i\theta} d\theta \int_0^\infty r dr \frac{2\sqrt{2}r^2}{\pi w(z)^4} e^{-\frac{2r^2}{w(z)^2}} e^{2i\psi} = \\ &= \frac{e^{i\alpha} e^{i\psi}}{\sqrt{2}w(z)} + \frac{e^{i\alpha} e^{i\psi}}{\sqrt{2}w(z)} - \frac{e^{i\alpha} e^{2i\psi}}{\sqrt{2}w(z)} = \frac{e^{i\alpha}}{\sqrt{2}w_0}. \end{aligned} \quad (22)$$

We can now write the effective Hamiltonian for this two populated modes as:

$$\hat{H}_I = \frac{i}{\sqrt{2}w_0} \left(e^{i\alpha} \hat{a}_{00}^\dagger \hat{a}_{01} - e^{-i\alpha} \hat{a}_{01}^\dagger \hat{a}_{00} \right). \quad (23)$$

We still need to evaluate $\sum_{k,l \in \mathcal{I}} [(f'_k | f'_l) - \sum_{j \in \mathcal{I}} (f'_k | f_j)(f_j | f'_l)]$ in order to calculate the sensitivity. From the angular parts of the integrals we obtain that the only non-zero terms are $(\partial LG_0^0 | \partial LG_0^0) - (\partial LG_0^0 | LG_0^1)(LG_0^1 | \partial LG_0^0)$ and $(\partial LG_0^1 | \partial LG_0^1) - (\partial LG_0^1 | LG_0^0)(LG_0^0 | \partial LG_0^1)$. After performing the corresponding integrals we get:

$$F_Q[\hat{\rho}(\delta_r)] = F_Q[\hat{\rho}, H_I] + \frac{2}{w_0^2} \left(\langle \hat{a}_{00}^\dagger \hat{a}_{00} \rangle_{\hat{\rho}} + 3 \langle \hat{a}_{01}^\dagger \hat{a}_{01} \rangle_{\hat{\rho}} \right). \quad (24)$$

Notice that the sensitivity does not depend on the angle of displacement α . This happens because of the cylindrical symmetry of the Laguerre-Gauss modes.

We can achieve quantum enhancements beyond the standard quantum limit on the estimation of a radial displacement by populating a pair LG_0^0 and LG_0^1 .

As each inner product presents a different double integral, it is much more difficult to calculate a general case with the LG modes than with the HG modes. With HG modes we achieved to study a case with arbitrary number of modes. Here, we will restrict ourselves to this two-mode scheme. Nevertheless, more difficult cases with more modes can be calculated in principle.

3.1.3 Analytical optimization of the sensitivity over all possible states

We have studied the sensitivity we can obtain in the estimation of a radial displacement with different mode structures and whether it can in principle outperform the SQL. This sensitivity, however is expressed always as a function of the state. Relevant questions would now be *Which is the state that achieves the maximal sensitivity? What is this optimal value?* We address these questions in this section.

Lemma 3.1. *The state $\hat{\rho}$ that achieves the maximum quantum Fisher information is pure.*

Proof: A mixed state is a convex combination of pure states $\hat{\rho}_{mix} = \sum_k p_k |\psi_k\rangle\langle\psi_k|$, with $\sum_k p_k = 1$, and the quantum Fisher information is a convex function. Then, $\max_{\rho} F_Q[\hat{\rho}(\theta)] = \max F_Q[\sum_i p_i |\psi_i\rangle\langle\psi_i|] \leq \sum_i p_i \max_{\psi_i} F_Q[|\psi_i\rangle\langle\psi_i|] \leq \max_{\psi} F_Q[|\psi\rangle\langle\psi|]$.

If $\hat{\rho}$ is a pure state we can simplify the expression 6. Notice that in this case $n = m = p_n = p_m = 1$:

$$F_Q[|\psi\rangle\langle\psi|, \hat{H}] := 4\langle\hat{H}^2\rangle_{\psi} - 8\frac{1}{2}|\langle\psi|\hat{H}|\psi\rangle|^2 = 4\langle(\Delta\hat{H})^2\rangle_{\psi}, \quad (25)$$

with $(\Delta\hat{H})^2$ the variance of \hat{H} . In all the studied cases where we can have quantum enhancements, a term $F_Q[\hat{\rho}, \hat{H}_I]$ appears on the expression of the sensitivity. With H_I the corresponding Hamiltonian. Now, if we want to optimize the sensitivity, we can substitute all these terms by variances:

$$\max_{\psi} F_Q[|\psi(\delta r)\rangle\langle\psi(\delta r)|] = \max_{\psi} \left[4\langle(\Delta\hat{H}_I)^2\rangle_{\psi} + \langle\text{linear terms}\rangle_{\psi} \right]. \quad (26)$$

The linear terms are the specific ones of each case. For example, in the radial displacement estimation with Laguerre modes (section 3.1.2) they are $2/w_0^2 \cdot (\langle\hat{a}_{00}^{\dagger}\hat{a}_{00}\rangle_{\psi} + 3\langle\hat{a}_{01}^{\dagger}\hat{a}_{01}\rangle_{\psi})$.

We will focus on the case where we have a constant number N of photons in our system. Then, we can create a complete basis for the Hilbert space of the quantum state, that labels the number of photons on each mode. This is $\{|k\rangle\}_{k=0}^N$ when we only have one populated mode, and $\{|k, N-k\rangle\}_{k=0}^N$ when we have two.

We can write an arbitrary pure state $|\psi\rangle$ of dimension $N+1$ in this basis as $|\psi\rangle = \sum_{k=0}^N c_k e^{i\phi_k} |k\rangle$. This are $2(N+1)$ parameters, but one of them is defined by the normalization condition, and another one by choosing a global phase. So we actually only need $2N$ free parameters to describe the state. We optimize the sensitivity over all states given a number of photons N . This is an optimization of a quadratic function over $2N$ parameters.

Different attempts were made to find an analytical solution for this problem with diverse optimization methods. The optimization was actually solved for $N=2$ and $N=3$. But the difficulty of the problem escalates rapidly with the number of photons and no general expression for an arbitrary N was found.

However, there is an elegant way to bypass this problem and find a quasi-optimal state. The idea is to optimize for all possible states only the quadratic part of the sensitivity (the variance of the effective Hamiltonian squared) forgetting about the linear terms. We call the state that maximizes this partial part of the sensitivity an approximate quasi-optimal state $|\tilde{\psi}_{opt}\rangle$. And we use it to calculate the full sensitivity in equation 26. The obtained result will not be optimal (as we are not taking the linear part into account in the optimization), but it will approach optimality as N increases. In this limit $N \gg 1$, the optimized quadratic term is much larger than the linear terms.

The maximum expectation value of the variance of an operator and the state that achieves this limit are [GLM06]:

$$\max_{\psi} \langle(\Delta\hat{H}_I)^2\rangle_{\psi} = \frac{|\lambda_{\max} - \lambda_{\min}|^2}{4} \quad \text{with} \quad |\psi_{opt}\rangle = \frac{|\lambda_{\max}\rangle + e^{i\varphi} |\lambda_{\min}\rangle}{\sqrt{2}} \quad (27)$$

Where λ_{\max} and λ_{\min} are the maximum and minimum eigenvalues of the effective Hamiltonian respectively and $|\lambda_{\max}\rangle$ and $|\lambda_{\min}\rangle$, the corresponding eigenstates. $|\psi_{\text{opt}}\rangle$ is optimal $\forall\varphi$. This knowledge will simplify the calculations.

At this point we will focus on mode parameter estimation strategies that achieve quantum enhancements on the estimation of a radial displacement. Notice that if we perform the displacement in the x direction ($\alpha = 0, \pi$) populating the pair HG_{00} and HG_{10} , or in y ($\alpha = \pi/2, 3\pi/2$) populating HG_{00} and HG_{01} , the Hamiltonian in equation 13 and sensitivity in 14 can be written as:

$$\hat{H}_I = \frac{i}{w_0} (\hat{a}^\dagger \hat{b} - \hat{b}^\dagger \hat{a}) \quad \text{and} \quad F_Q[\hat{\rho}(\delta r)] = F_Q[\hat{\rho}, \hat{H}_I] + \frac{8}{w_0^2} \langle \hat{b}^\dagger \hat{b} \rangle_{\hat{\rho}} \quad (28)$$

Where $\hat{a}^{(\dagger)}$ and $\hat{b}^{(\dagger)}$ are the creation and destruction operators on the ground and the exited modes respectively. The equations in 28 are very similar to the Hamiltonian of the radial displacement in an arbitrary direction with the first two populated LG modes (expression 23) and the corresponding sensitivity 24. They can all be written as $\hat{H}_I = c\hat{a}^\dagger \hat{b} + c^* \hat{a} \hat{b}^\dagger$, and $F_Q = 4\langle (\Delta \hat{H}_I^2) \rangle_{\tilde{\psi}} + d_1 \langle \hat{N}_a \rangle_{\tilde{\psi}} + d_2 \langle \hat{N}_b \rangle_{\tilde{\psi}}$. With $\hat{N}_a = \hat{a}^\dagger \hat{a}$ and $\hat{N}_b = \hat{b}^\dagger \hat{b}$ the number operators on each mode. The displacements with HG have $c = i/w_0$, $d_1 = 0$ and $d_2 = 8/w_0^2$; and with LG $c = ie^{i\alpha}/\sqrt{2}w_0$, $d_1 = 2/w_0^2$ and $d_2 = 6/w_0^2$. We will optimize this general case. Firstly, notice the Hamiltonian can be rewritten in the number of photons basis as:

$$\hat{H}_I = \sum_{k=0}^N \sqrt{(k+1)(N-k)} (c|k+1, N-k-1\rangle\langle k, N-k| + h.c.), \quad (29)$$

with h.c. the hermitian conjugate of the first term. This Hamiltonian has to be diagonalized in order to find the maximum possible value of its variance, and apply the quasi-optimal procedure. We can do it in general as it is very symmetric. We obtain the set of eigenvalues $\{\lambda_i\}_{i=0}^N = \{-N|c|, (2-N)|c|, \dots, (N-2)|c|, N|c|\}$. The spread is $2N|c|$, so the maximum expectation value that can be achieved according to equation 27 is $N^2|c|^2$.

In order to find the optimal state, we only need to calculate the eigenvectors corresponding to the maximum and minimum eigenvalues: $(H_I \pm N|c|\mathbb{1})|\tilde{x}\rangle = 0$. We find that the eigenvectors have binomially distributed coefficients:

$$\begin{aligned} |\lambda_{\max}\rangle &= \frac{1}{\sqrt{2^N}} \sum_{k=0}^N \sqrt{\frac{(c^*)^k}{c^k} \binom{N}{k}} |N-k, k\rangle \\ |\lambda_{\min}\rangle &= \frac{1}{\sqrt{2^N}} \sum_{k=0}^N (-1)^k \sqrt{\frac{(c^*)^k}{c^k} \binom{N}{k}} |N-k, k\rangle. \end{aligned} \quad (30)$$

The superposition of these two eigenvectors with any phase will give us the quasi-optimal state. Notice that by choosing $\varphi = 0$ in equation 27 all the odd terms cancel, so we can write the quasi-optimal state as:

$$|\tilde{\psi}_{\text{opt}}\rangle = \frac{1}{\sqrt{2^{N-1}}} \sum_{k=0}^{\lfloor N/2 \rfloor} \sqrt{\frac{(c^*)^{2k}}{c^{2k}} \binom{N}{2k}} |N-2k, 2k\rangle. \quad (31)$$

With $\lfloor x \rfloor$ the floor function (it takes the greatest integer smaller or equal to x). This state has the property $\langle \hat{H}_I \rangle_{\tilde{\psi}} = 0$. We calculate now the sensitivity in equation 28. The result will be an approximate quasi-maximal sensitivity. We find:

$$F_Q[|\tilde{\psi}_{\text{opt}}\rangle\langle\tilde{\psi}_{\text{opt}}|] = 4N^2|c|^2 + \frac{d_1 + d_2}{2}N \quad (32)$$

Notice that this sensitivity does indeed scale quadratically with the number of photons. We expect that it will be closer and closer to the absolute optimal as N increases. This fact will be checked numerically in section 3.1.5 (figures 4 and 5).

Our analytical quasi-optimal state 31 achieves a quasi-maximal quantum enhanced sensitivity 32 beyond the SQL.

3.1.4 Quasi-optimal state for transverse displacements as a rotated NOON

We have calculated explicitly an analytical quasi-optimal state 31. Now, we are going to give a more intuitive expression for it through the **Schwinger representation** [CMM⁺06]. The main idea is to rewrite our general effective Hamiltonian $\hat{H}_I = c\hat{a}^\dagger\hat{b} + c^*\hat{a}\hat{b}^\dagger$ as a spin-like Hamiltonian and manipulate it as such. The excited and ground mode will be treated as the up and down spin using the two-mode bosonic representation of the SU(2) algebra [Sch00]. The angular momentum operators are:

$$\hat{J}_x = \frac{\hat{a}^\dagger\hat{b} + \hat{b}^\dagger\hat{a}}{2} \quad \hat{J}_y = \frac{\hat{a}^\dagger\hat{b} - \hat{b}^\dagger\hat{a}}{2i} \quad \hat{J}_z = \frac{\hat{a}^\dagger\hat{a} - \hat{b}^\dagger\hat{b}}{2}. \quad (33)$$

This allows us to write our effective Hamiltonian as $\hat{H}_I = 2[\text{Re}(c)\hat{J}_x - \text{Im}(c)\hat{J}_y]$. Defining the normalized vector $\vec{n} := (\text{Re}(c), -\text{Im}(c), 0)/|c|$ we can write $\hat{H}_I = 2|c|\hat{J}_{\vec{n}}$. With $\hat{J}_{\vec{n}} = \vec{n} \cdot \vec{J}$, and $\vec{J} = (\hat{J}_x, \hat{J}_y, \hat{J}_z)$. Notice that the vector $\vec{m} = (\text{Im}(c), \text{Re}(c), 0)/|c|$ defines a $\hat{J}_{\vec{m}}$ that is orthogonal to both $\hat{J}_{\vec{n}}$ and \hat{J}_z . Therefore, a rotation $\hat{U} = \exp(-i\pi\hat{J}_{\vec{m}}/2)$ will bring elements from the canonical \hat{J}_z basis to the Hamiltonian $\hat{J}_{\vec{n}}$ basis.

Let us optimize now the quadratic part of the sensitivity like in the previous section. We can do it now in a much more elegant way by working in the canonical \hat{J}_z basis, and then performing the above-defined rotation \hat{U} to obtain the information in the Hamiltonian $\hat{J}_{\vec{n}}$ basis. We know (equations 27) that the maximum value $\langle(\Delta\hat{H}_I)^2\rangle_\psi$ can achieve is the spread of the extreme eigenvalues squared divided by 4.

The rotated Hamiltonian $\hat{H}_z = 2|c|\hat{J}_z$ is already diagonal so the set of eigenvalues is trivially: $2|c|\{\frac{N}{2}, \frac{N}{2} - 1, \dots, 1 - \frac{N}{2}, -\frac{N}{2}\}$. The eigenvalues of an operator do not change under rotation so these are actually the eigenvalues of our effective Hamiltonian \hat{H}_I . The spread is $2N|c|$, so the maximum value that the variance of the Hamiltonian can achieve is $\max\langle(\Delta\hat{H}_I)^2\rangle_\psi = N^2|c|^2$. This coincides with the result in the previous section.

The eigenstates corresponding to the maximum and minimum eigenvalues of \hat{J}_z are $|0, N\rangle$ and $|N, 0\rangle$. Therefore, the quasi-optimal state for the rotated Hamiltonian \hat{H}_z is the NOON state in the \hat{J}_z basis:

$$|\tilde{\psi}\rangle_z = |NOON\rangle_z = \frac{|N, 0\rangle_z + e^{i\varphi}|0, N\rangle_z}{\sqrt{2}}, \quad \forall\varphi. \quad (34)$$

In order to get the quasi-optimal state of the original Hamiltonian \hat{H}_I we have to perform the rotation \hat{U} . This allows us to write compactly:

$$|\tilde{\psi}_{\text{opt}}\rangle = U|\tilde{\psi}\rangle_z = U|NOON\rangle_z. \quad (35)$$

We can interpret our quasi-optimal state as a rotated NOON state, with $\hat{U} = \exp(-i\pi\hat{J}_{\vec{m}}/2)$ the rotation operator.

We further checked numerically that this state is indeed equivalent to the one we obtained in 31, they both return the same sensitivity. The code is provided in Appendix A.

3.1.5 Numerical optimization of transverse displacements

There is a less obvious but better way to perform the optimization. It is based on the intuition that our optimal state should have the property $\langle \hat{H}_I \rangle_\psi \sim 0$. This is not unfounded: Notice that the sensitivity can be written as $F_Q = 4\langle \hat{H}_I^2 \rangle_\psi - 4\langle \hat{H}_I \rangle_\psi^2 + d_1\langle \hat{N}_a \rangle_\psi + d_2\langle \hat{N}_b \rangle_\psi$, so it makes sense that we would want the negative term to be small (or ideally zero) if we are trying to maximize the function. Also, we have seen that the quasi-optimal state in 31 indeed has this property.

Lemma 3.2. *Let the state $|\psi\rangle$ maximize $\max_\varphi[\langle \hat{H}_1^2 + \hat{H}_2 \rangle_\varphi] = \langle \hat{H}_1^2 + \hat{H}_2 \rangle_\psi$. Then, there is an upper bound in the function $\max_\varphi[\langle \hat{H}_1^2 + \hat{H}_2 \rangle_\varphi - \langle \hat{H}_1 \rangle_\varphi^2] \leq \langle \hat{H}_1^2 + \hat{H}_2 \rangle_\psi$. The inequality is saturated if and only if $\langle \hat{H}_1 \rangle_\psi = 0$*

Proof: Notice $\max_\varphi[\langle \hat{H}_1^2 + \hat{H}_2 \rangle_\varphi - \langle \hat{H}_1 \rangle_\varphi^2] \leq \max_\varphi[\langle \hat{H}_1^2 + \hat{H}_2 \rangle_\varphi] = \langle \hat{H}_1^2 + \hat{H}_2 \rangle_\psi$ and the inequality is saturated if and only if $\langle \hat{H}_1 \rangle_\psi = 0$

If we let $\hat{H}_I = \hat{H}_1$, and $d_1\langle \hat{N}_a \rangle_\psi + d_2\langle \hat{N}_b \rangle_\psi = \hat{H}_2$, this lemma applies to our case. The strategy will be to find the state $|\psi\rangle$ that maximizes $\max_\varphi[\langle \hat{H}_I^2 + d_1\hat{N}_a + d_2\hat{N}_b \rangle_\varphi]$ and then calculate $\langle \hat{H}_I \rangle_\psi$. If we find $\langle \hat{H}_I \rangle_\psi \neq 0$ we will have a new approximation for our sensitivity that will be compared to the quasi-optimal one found in equation 32. If we find $\langle \hat{H}_I \rangle_\psi = 0$, according to the lemma 3.2, the state $|\psi\rangle$ will maximize the sensitivity, so we will be able to calculate the actual optimal sensitivity value.

The maximization is solved by the eigenvector corresponding to the maximum eigenvalue of $\hat{H}_I^2 + d_1\hat{N}_a + d_2\hat{N}_b$. However, diagonalizing this operator analytically for arbitrary constants is a difficult task, and it gets more and more challenging when N increases. This is the reason why this procedure has been done numerically.

The *optimal state code* in appendix B performs this diagonalization numerically and checks whether the condition $\langle \hat{H}_I \rangle_\psi = 0$ is fulfilled. We find that it is actually fulfilled for the constants c , d_1 and d_2 in our problems and for all N . This means that the sensitivity provided by the code is indeed the maximal sensitivity that can be obtained with the given setting. The code also outputs the optimal state and the POVM that realizes the optimal measurement in the number of photons basis we defined in section 3.1.3.

We have found numerically the maximal sensitivity that can be achieved in the estimation of a transverse displacement in the x or y -axis when populating the first two HG modes, and in the estimation of a radial displacement when populating the first two LG modes. We also know the state that achieves it.

At this point two questions arise: *Which is the relation between the optimal sensitivity we have found numerically and the quasi-optimal sensitivity we have found analytically? And which is the relation between the optimal and quasi-optimal states that achieve these sensitivities?*

In order to answer the first question let us plot the optimal and quasi-optimal sensitivities for different values of N . This plot is shown in figures 4 and 5 with the constants of the radial displacement estimation with two Laguerre mode. A very similar plot is obtained for the x and y -axis displacement with the first two Hermite modes. These similar plots and the used code can be seen in the appendix C.

In the first plot (figure 4) we see that both lines are close and actually getting closer with increasing N . In fact, for values $N > 5$ the two lines can no longer be visually distinguished on this scale. From figure 5 we observe that the difference between the quasi-optimal and the optimal sensitivity gets smaller with an increasing number of photons

and stabilizes in the limit $N \gg 1$ around $0.5w_0^2$, while F_Q grows quadratically. This means that the weighted difference between the quasi-optimal and optimal sensitivity decreases quadratically with the number of photons.

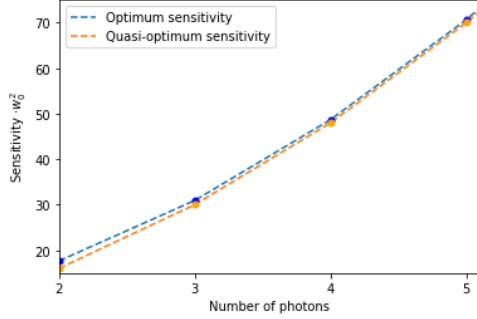


Figure 4: Comparison of the optimal and quasi-optimal sensitivities as a function of N

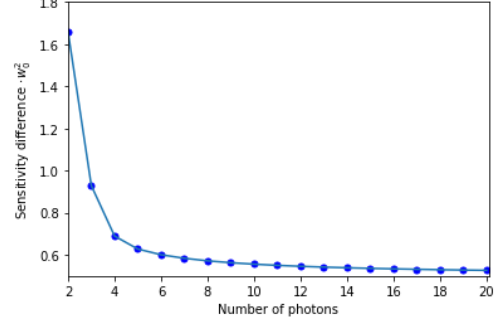


Figure 5: Difference between the optimal and quasi-optimal sensitivities as a function of N

This proves that the analytical expressions for the quasi-optimal sensitivity (expression 32) and the state (31) that achieves it are very good approximations of the absolute optimal values.

Intuitively, we expect the numerical optimal state to be very similar to the quasi-optimal analytical state in equation 31. We are going to make use again of the Schwinger representation, rotating our state to the \hat{J}_z basis. The reason why we do this is because it will be easier to compare the optimal state with the NOON state (that has only two elements, the extremes of the basis) than with the complex quasi-optimal state 31 with lots of binomial distributed terms.

The results confirm the intuition: the numerical obtained optimal state is indeed a composition of the NOON state (the rotated quasi-optimal) and other "NOON-like" states:

$$|\psi_{\text{opt}}\rangle_z = c_0 \frac{|N0\rangle_z + |0N\rangle_z}{\sqrt{2}} + c_1 \frac{|N-1, 1\rangle_z + |1, N-1\rangle_z}{\sqrt{2}} + c_2 \frac{|N-2, 2\rangle_z + |2, N-2\rangle_z}{\sqrt{2}} + \dots \quad (36)$$

With $c_i^2 = p_i$ the population of each of these NOON states, and the property $\sum_i p_i = 1$. We will call the second term *Secondary NOON*, the third *Tertiary NOON*, and so on. We see that the population p_0 of the regular NOON state grows with N and asymptotically approaches 1. Consequently, the population of the other NOONs decreases and asymptotically approach 0. Moreover, we see that $p_0 > p_1 > p_2 > \dots$. The next figures show the population of the NOON states as a function of N :

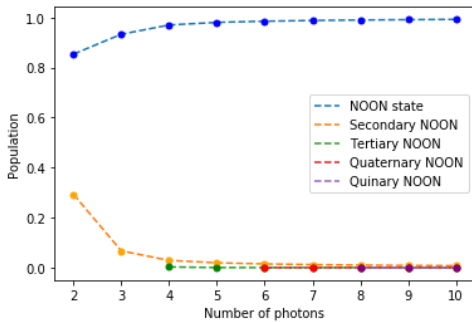


Figure 6: Population of the NOON states as a function of N

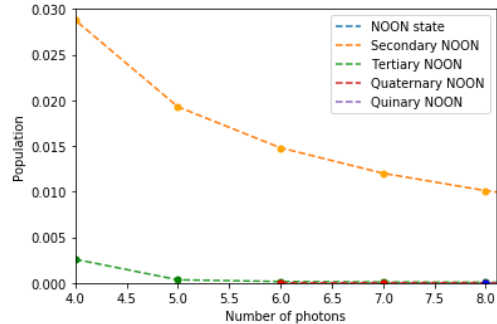


Figure 7: Zoom on Figure 6 to appreciate the decrease of the secondary and tertiary NOONs

We see how, indeed, the optimal state is very similar to the quasi-optimal (the NOON), and it gets closer to it asymptotically with increasing number of photons. We can interpret the secondary NOONs as the corrections to the quasi-optimal state due to the linear terms. The code used to plot these figures can be found in appendix D.

3.1.6 Application: Displacement on an arbitrary direction

Imagine that we want to estimate a radial displacement of light with quantum enhanced sensitivity. Ideally we would prefer to use a fundamental Gaussian beam, because it is the easiest to produce in the lab. That is, we would desire to populate the mode HG_{00} or LG_0^0 (remember that they both represent a fundamental Gaussian mode in Cartesian or polar coordinates respectively). However, as we have deduced in sections 3.1.1 and 3.1.2, we can not obtain quantum enhancements on the estimation of a radial displacement populating just a single mode.

We have to use at least a two-mode strategy. It is still desirable that one of the modes is a Gaussian beam, so the questions to answer are: *Which additional mode can we populate to obtain quantum enhancements? From the different possible strategies, which will produce the best sensitivity?* By analyzing the derivatives of the HG modes (equation 11) we deduced that, in order to get quantum enhancements, we need to populate at least two contiguous modes. The only modes contiguous to HG_{00} are HG_{01} and HG_{10} (a superposition of these two excited modes $\cos \alpha HG_{10} + \sin \alpha HG_{01}$ can also produce enhancements). We also have learned from section 3.1.2 b), that we can obtain quantum enhancements with the LG modes by populating the pair LG_0^0 and LG_0^1 . We investigate the following strategies:

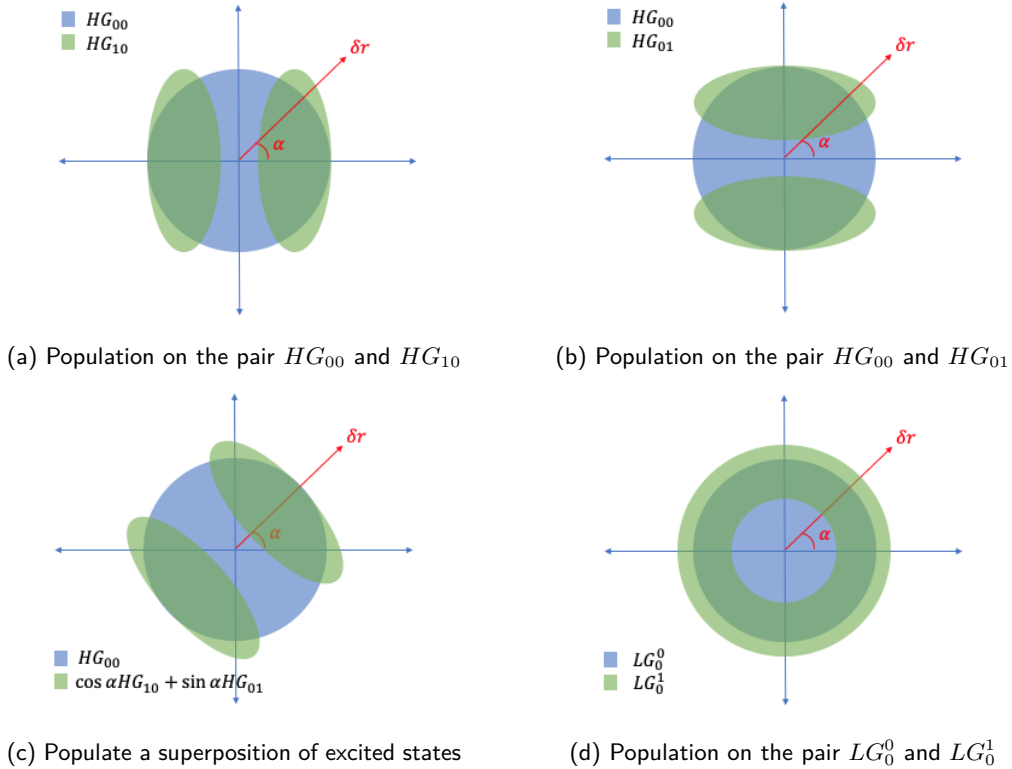


Figure 8: Four different possible strategies.

This is just a visual representation of the superposed modes. The actual shape of the superposed modes can be seen in appendix F. The sensitivity for the two-mode LG

strategy is given in equation 24, with the corresponding effective Hamiltonian in equation 23. And the sensitivities for the two-mode HG strategies are particular cases of equation 14, explicitly:

$$\begin{aligned}
F_Q^{HG_{10}}[|\psi(\delta_r)\rangle] &= F_Q[\psi, \hat{H}_I^{HG_{10}}] + \frac{4}{w_0^2} \left(\sin(\alpha)^2 \langle \hat{a}_{00}^\dagger \hat{a}_{00} \rangle_\psi + (1 + \cos(\alpha)^2) \langle \hat{a}_{01}^\dagger \hat{a}_{01} \rangle_\psi \right), \\
F_Q^{HG_{01}}[|\psi(\delta_r)\rangle] &= F_Q[\psi, \hat{H}_I^{HG_{01}}] + \frac{4}{w_0^2} \left(\cos(\alpha)^2 \langle \hat{a}_{00}^\dagger \hat{a}_{00} \rangle_\psi + (1 + \sin(\alpha)^2) \langle \hat{a}_{10}^\dagger \hat{a}_{10} \rangle_\psi \right), \quad (37) \\
\text{with } \hat{H}_I^{HG_{10}} &= \frac{i \cos \alpha}{w_0} \left[\hat{a}_{00}^\dagger \hat{a}_{10} - \hat{a}_{10}^\dagger \hat{a}_{00} \right] \quad \text{and} \quad \hat{H}_I^{HG_{01}} = \frac{i \sin \alpha}{w_0} \left[\hat{a}_{00}^\dagger \hat{a}_{01} - \hat{a}_{01}^\dagger \hat{a}_{00} \right].
\end{aligned}$$

We focus on the scenario where we do not know the direction of the displacement. Notice that, due to the symmetry of the LG modes, the sensitivity in equation 24 is constant $\forall \alpha$. But this is not the case in the HG strategies (notice that the sensitivities in 37 depend on α). We wonder which strategy is better on average. Let us plot the different strategies as a function of the angle. $\forall N$ the shape of the functions is:

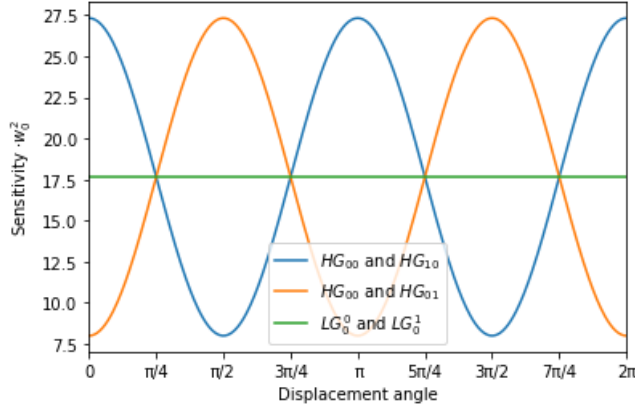


Figure 9: Maximal sensitivity achieved by LG and two different HG schemes

The functions have the expected behaviour. The HG strategies are better than the LG in some intervals, but worse in some others. In fact, it can be calculated that, on average, both strategies achieve the same sensitivity for each N . So, if we don't have any information about the most probable direction of displacement, both strategies are equally good on average. If our desire is to have the best sensitivity in the worst-case scenario, then the LG modes are better as $\min_\alpha F_Q^{LG} > \min_\alpha F_Q^{HG}$, for all HG strategies. The code in appendix E outputs the figure 9 and compares the average sensitivity between the strategies.

We have already seen in section 3.1.3 that the maximum sensitivity that can be obtained with the strategy in figure 8a is achieved for a displacement along the x -axis, and the maximum sensitivity that can be obtained with the strategy in figure 8b is achieved for a displacement along the y -axis. The shape of both sensitivity functions is actually the same up to a rotation of $\pi/2$ in the x - y plane and provided in equation 28. We expect there to be a mode scheme which achieves this same maximum sensitivity for a displacement in α . Indeed the scheme $HG_{\text{mix}} = \cos \alpha HG_{10} + \sin \alpha HG_{01}$ in figure 8c returns:

$$\begin{aligned}
F_Q^{HG_{\text{mix}}}[|\psi(\delta_r)\rangle] &= F_Q[\psi, \hat{H}_I^{\text{mix}}] + \frac{8}{w_0^2} \langle \hat{a}_{\text{mix}}^\dagger \hat{a}_{\text{mix}} \rangle_\psi \\
\text{With } \hat{H}_I^{HG_{\text{mix}}} &= \frac{i}{w_0} \left[\hat{a}_{00}^\dagger \hat{a}_{\text{mix}} - \hat{a}_{\text{mix}}^\dagger \hat{a}_{00} \right], \quad (38)
\end{aligned}$$

This state will achieve the best results if we know the direction of the displacement. Actually it is quite obvious that the schemes in 8a, 8b, and 8c would achieve the same sensitivities for a displacement in x , y , and α respectively, because we can see this three cases just as a rotation of the axis.

If we know the direction of displacement the best strategy is to populate HG_{00} and HG_{mix} . However, if the direction is random HG and LG strategies will give us the same results in average. LG modes provide an advantage in the worst-case scenario because they have a higher minimum possible sensitivity.

3.2 Estimation of a change on the wavelength

In this section we will work in the Hermite-Gauss mode basis. We will start by noticing in section 3.2.1 that we can achieve quantum enhancements populating just a single mode. In section 3.2.2 we will see another setting that can achieve even better sensitivities. We will find a quasi-optimal analytical state for the single mode case in section 3.2.3, and check that it is a good approximation to the optimal in section 3.2.4.

3.2.1 We populate a single arbitrary Hermite mode

Using the recurrence relations in 10 and some algebra¹, we can express the derivative of an arbitrary HG_{nm} mode with respect to the wavelength as a sum of different Hermite-Gauss modes:

$$\left. \frac{\partial HG_{nm}}{\partial \delta \lambda} \right|_{\delta \lambda=0} = -\frac{iz}{4\pi w_0^2} \left[\sqrt{(n+1)(n+2)} HG_{n+2,m} + \sqrt{(m+1)(m+2)} HG_{n,m+2} + \sqrt{n(n-1)} HG_{n-2,m} + \sqrt{m(m-1)} HG_{n,m-2} \right] + \left[\frac{iz}{2\pi w_0^2} (n+m+1) + \frac{2\pi iz}{\lambda^2} \right] HG_{nm}. \quad (39)$$

Notice that the mode is not orthogonal to its derivative due to the last term in equation 39. Therefore, the effective Hamiltonian will not vanish even if we populate a single HG_{nm} .

$$\hat{H}_I = i(HG_{nm} | \partial HG_{nm}) \hat{a}_{nm}^\dagger \hat{a}_{nm} = -z \left[\frac{n+m+1}{2\pi w_0^2} + \frac{2\pi}{\lambda^2} \right] \hat{a}_{nm}^\dagger \hat{a}_{nm}, \quad (40)$$

and we will find quadratic scaling on the sensitivity:

$$F_Q[\hat{\rho}(\delta \lambda)]_{\delta \lambda=0} = F_Q[\hat{H}_I, \hat{\rho}] + \frac{z^2}{2\pi^2 w_0^4} \left[n^2 + n + 1 + m^2 + m + 1 \right] \langle \hat{N}_{nm} \rangle_{\hat{\rho}}. \quad (41)$$

We can achieve quantum enhancements beyond the standard quantum limit for the estimation of the wavelength by populating a single HG_{nm} mode.

3.2.2 We populate a pair HG_{00} and $(HG_{02} + HG_{20})/\sqrt{2}$

Even though we have quantum enhancements in the simplest case of populating a single mode, analyzing the structure of the mode derivative with respect to the parameter, we observe that we can get even better sensitivity by increasing the overlap between

¹It is important to notice that all terms involving z_R or k have to be derived as they depend on the wavelength. This affects all terms in the mode (expression 9) except the normalization constant

the populated modes and their derivatives (remember Figure 1). This can be done by populating a second mode $HG_{\text{mix}} = (HG_{02} + HG_{20})/\sqrt{2}$. Now, the derivatives of HG_{00} and HG_{mix} both contain HG_{00} and HG_{mix} terms. We have:

$$\begin{aligned}
1. \quad & \left. \frac{\partial HG_{00}}{\partial \delta \lambda} \right|_{\delta \lambda=0} = -\frac{iz}{2\pi w_0^2} HG_{\text{mix}} + \left(\frac{iz}{2\pi w_0^2} + \frac{2\pi iz}{\lambda^2} \right) HG_{00} \\
2. \quad & \left. \frac{\partial HG_{\text{mix}}}{\partial \delta \lambda} \right|_{\delta \lambda=0} = \left(\frac{3iz}{2\pi w_0^2} + \frac{2\pi iz}{\lambda^2} \right) HG_{\text{mix}} - \\
& - \frac{iz}{4\pi w_0^2} \left(\sqrt{6}(HG_{04} + HG_{40}) + 2HG_{22} + 2HG_{00} \right).
\end{aligned} \tag{42}$$

Therefore the Hamiltonian and the sensitivity read:

$$\begin{aligned}
\hat{H}_I &= - \left(\frac{z}{2\pi w_0^2} + \frac{2\pi z}{\lambda^2} \right) a_{00}^\dagger a_{00} + \frac{z}{2\pi w_0^2} a_{\text{mix}}^\dagger a_{00} - \\
& - \left(\frac{3z}{2\pi w_0^2} + \frac{2\pi z}{\lambda^2} \right) a_{\text{mix}}^\dagger a_{\text{mix}} + \frac{z}{2\pi w_0^2} a_{00}^\dagger a_{\text{mix}} \\
F_Q[\hat{\rho}(\delta \lambda)]_{\delta \lambda=0} &= F_Q[\hat{H}_I, \hat{\rho}] + \frac{4z^2}{\pi^2 w_0^4} \langle \hat{N}_{\text{mix}} \rangle \hat{\rho}.
\end{aligned} \tag{43}$$

This sensitivity will scale better than the one with a single populated mode (equation 41), as we have increased the term that scales quadratically.

Notice that for simplicity we have used $HG_{nm} = HG_{00}$. But we could improve the scaling even further by choosing a pair HG_{nm} and $(HG_{n+2,m} + HG_{n-2,m} + HG_{n,m+2} + HG_{n,m-2})/2$. This way, we would take even better advantage of the structure of the mode derivative.

3.2.3 Optimization of the sensitivity in wavelength variations

In the case where we only populate a single HG_{nm} the Hamiltonian is already diagonal, in the eigenbasis of the number operator, as the effective Hamiltonian coincides with \hat{N}_{nm} up to a constant that depends on the mode indices: $\hat{H}_I = -k(n, m)\hat{N}_{nm}$. Therefore it is an easy task to calculate the quasi-optimal state and sensitivity using equations 27:

$$\begin{aligned}
F_Q \left[\left| \tilde{\psi}_{\text{opt}} \right\rangle \left\langle \tilde{\psi}_{\text{opt}} \right| \right] &= z^2 N^2 \left[\frac{n+m+1}{2\pi w_0^2} + \frac{2\pi}{\lambda^2} \right]^2 + \frac{z^2 N}{4\pi^2 w_0^4} \left[n^2 + m^2 + n + m + 2 \right] \\
\left| \tilde{\psi}_{\text{opt}} \right\rangle &= \frac{|N\rangle + e^{i\varphi} |0\rangle}{\sqrt{2}}; \quad \forall \varphi.
\end{aligned} \tag{44}$$

In the following, we will study the quality of this quasi-optimal state with a numerical program.

3.2.4 Numerical analysis of the quasi-optimal procedure in the estimation of a wavelength displacement

We note from equation 44 that as the indices of the mode increase, the constant multiplying the quadratic factor grows faster than the constant multiplying the linear term. This means that for excited modes, our quasi-optimal state approaches to the optimal. Let us consider scenario of lowest quadratic scaling on the sensitivity where the populated mode is HG_{00} . Using $\lambda z_R = w_0^2 \pi$ we can rewrite the quasi-optimal sensitivity as:

$$F_Q \left[\left| \tilde{\psi}_{\text{opt}} \right\rangle \left\langle \tilde{\psi}_{\text{opt}} \right| \right] = z^2 N^2 \left[\frac{1}{4z_R^2 \lambda^2} + \frac{2}{z_R \lambda^3} + \frac{4\pi^2}{\lambda^4} \right]^2 + \frac{z^2 N}{2z_R^2 \lambda^2}. \tag{45}$$

For simplicity let us call A the constant multiplying the quadratic term, and B the constant multiplying the linear one. Let us analyze the two extreme cases. When $z_R \gg \lambda$, we have $A \gg B$. The quadratic term is much larger, then the quasi-optimal state will be near the optimal. However, when $z_R \ll \lambda$ we find $2A \simeq B$. Again, let us focus on this worst case scenario and perform a numerical process to assess the quality of our quasi-optimal state.

The process will consist in generating 100.000 random states for $N \in [2, 6]$, and calculating for each one the sensitivity. We will choose the maximum from this 100.000 calculations and compare it with our quasi-optimal sensitivity. This process loses effectiveness when N increases (as the probability of randomly choosing a state better than the quasi-optimal one decreases). On the other hand, we also know that our $|\tilde{\psi}_{\text{opt}}\rangle$ gets better as N increases. We obtain the following plot (the used code can be seen in appendix G):

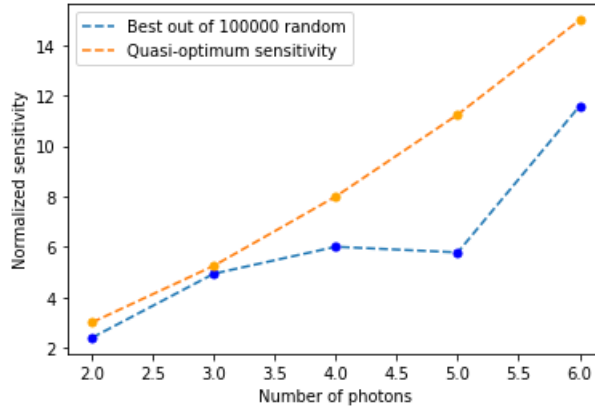


Figure 10: Comparison of the quasi-optimal state 44 and the best out of 100.000 random states

Even in the scenario where the quasi-optimal state is expected to perform more poorly, none of the 100.000 randomly generated states for each N achieves a better sensitivity.

The NOON state achieves to a very good approximation the maximal sensitivity that can be obtained in the estimation of the wavelength (equation 44).

4 Conclusions

In this master thesis we have exhaustively studied analytically and numerically the limits on the estimation of different quantum parameters using diverse mode bases and schemes. Each case has been analyzed in order to determine whether it is possible to achieve quantum enhanced sensitivity beyond the standard quantum limit. Analytical calculations have resulted in a quasi-optimal state and the corresponding quasi-maximal sensitivity. Numerical and analytical efforts have been deployed to demonstrate that this quasi-optimal state is a very good approximation of the actual optimal. For some of the studied systems the optimal state has been found and analyzed numerically. The obtained knowledge has been applied to identify suitable strategies for the problem of beam positioning with an unknown displacement axis. Let us sum them up this results:

- a) *Estimation of the sensitivity of a radial displacement on a given direction populating a single HG_{nm} or LG_p^m mode:* No quantum enhancement can be found beyond the standard quantum limit.

- b) *Estimation of the sensitivity of a radial displacement populating the first two HG and LG modes:* We can have quantum enhancements beyond the SQL. We have an analytical quasi-optimal state (equation 31), and a numerical optimal state that can be found using the code in appendix B. Using this code we can also output an optimal POVM.
- c) *Theoretical interpretation of the optimal state found in the radial displacements:* The quasi-optimal state can be interpreted as a rotated NOON state. The linear terms in the sensitivity generate secondary NOON corrections that appear in the numerical optimal state (equation 36). As the number of photons increase, the population of the primary NOON approaches rapidly to 1, and the population of the secondary NOONs goes to 0, so our quasi-optimal state asymptotically converges to the optimal one.
- d) *Optimization of the best mode scheme that can be used to estimate a radial displacement:* We have seen in section 3.1.6 that, if we know the direction of displacement, an HG mode strategy will provide a better sensitivity. If the direction is random, HG and LG strategies provide the same sensitivity in average. LG provide an advantage for the "worst-case scenario" sensitivity, as they have a higher minimum possible value of F_Q over α .
- e) *Estimation of the sensitivity of wavelength variations populating a single HG_{nm} :* We can have quantum enhancements beyond the SQL. We have calculated an analytical quasi-optimal state and the corresponding quasi-maximal sensitivity (equation 44). It has been checked numerically (section 3.2.4) that it is a very good approximation of the actual optimum.
- f) *Estimation of the sensitivity of wavelength variation populating a pair HG_{00} and $(HG_{20} + HG_{02})/\sqrt{2}$:* We can achieve quantum enhanced sensitivity beyond the SQL and beyond the single-mode scheme with HG_{00} .

With these new results we can say that the objectives of the project have been fulfilled.

A particularly challenging problem turned out to be the derivative of the Laguerre-Gauss basis. Since the orthonormality condition could not be used in the same way as in the HG case, we were not able to identify the quantum limits with the desired level of generality. Nevertheless, relevant results have been found for simple, low-mode scenarios and the path has been laid to calculate more challenging schemes via the solution of demanding integrals.

Moreover, within the time frame of this Master's thesis we were not able to find the optimal state that maximizes the sensitivity analytically. Different arduous optimization methods and numerical machinery were deployed to this endeavor. Results were found for small numbers of photons, but no general solution was discovered for an arbitrary number of photons. However, the optimal state has been obtained numerically (section 3.1.5), and interpreted analytically. And we also provided numerical evidence suggesting that the analytical quasi-optimal state achieves very good results.

This project opens the door to new questions that will have to be studied in the future: *Is there an analytical way to find the state that optimizes the sensitivity for an arbitrary mode scheme?* The obtained states that achieve better sensitivities are usually very challenging to create and analyze in a laboratory, *Which is the trade off between the theory and the application?* *Can we find manipulable states that achieve quasi-optimal sensitivity?*

All this questions and more will be addressed on the following months but fall beyond this Master's thesis.

Bibliography

- [BC94] Samuel L. Braunstein and Carlton M. Caves. Statistical distance and the geometry of quantum states. *Phys. Rev. Lett.*, 72, 1994.
- [BRSR15] B. Brecht, Dileep V. Reddy, C. Silberhorn, and M. G. Raymer. Photon temporal modes: A complete framework for quantum information science. *Phys. Rev. X*, 5, 2015.
- [CFB⁺13] Ludovico Carbone, Paul Fulda, Charlotte Bond, Frank Brueckner, Daniel Brown, Mengyao Wang, Deepali Lodhia, Rebecca Palmer, and Andreas Freise. The generation of higher-order laguerre-gauss optical beams for high-precision interferometry. *Journal of visualized experiments*, 2013.
- [CMM⁺06] S. Chaturvedi, G. Marmo, N. Mukunda, R. Simon, and A. Zampini. The Schwinger representation of a group: concept and applications. *Reviews in Mathematical Physics*, 18(08), 2006.
- [Cra99] Harald Cramér. Mathematical methods of statistics (pms-9). *Princeton University Press*, 1999.
- [Fis22] Ronald A Fisher. On the mathematical foundations of theoretical statistics. *Philosophical transactions of the Royal Society of London*, 222, 1922.
- [FT20] C. Fabre and N. Treps. Modes and states in quantum optics. *Rev. Mod. Phys.*, 92, 2020.
- [GLM06] Vittorio Giovannetti, Seth Lloyd, and Lorenzo Maccone. Quantum metrology. *Physical review letters*, 96(1), 2006.
- [GLM11] Vittorio Giovannetti, Seth Lloyd, and Lorenzo Maccone. Advances in quantum metrology. *Nature photonics*, 5(4), 2011.
- [GTF22] Manuel Gessner, Nicolas Treps, and Claude Fabre. Quantum limits on mode parameter estimation. *arXiv*, 2022.
- [Hel69] Carl W Helstrom. Quantum detection and estimation theory. *Journal of Statistical Physics*, 1(2), 1969.
- [Hol11] Alexander S Holevo. Probabilistic and statistical aspects of quantum theory. *Springer Science & Business Media*, 1, 2011.
- [MMLO⁺15] Mohammad Mirhosseini, Omar S Magaña-Loaiza, Malcolm N O’Sullivan, Brandon Rodenburg, Mehul Malik, Martin P J Lavery, Miles J Padgett, Daniel J Gauthier, and Robert W Boyd. High-dimensional quantum cryptography with twisted light. *New Journal of Physics*, 17(3), 2015.
- [PS14] Luca Pezzé and Augusto Smerzi. Quantum theory of phase estimation. *Atom Interferometry*, 188, 2014.
- [Rao92] C. Radhakrishna Rao. Information and the accuracy attainable in the estimation of statistical parameters. *Springer New York*, 1992.
- [Sch00] Julian Schwinger. On angular momentum. *World Scientific*, 2000.
- [TA14] Géza Tóth and Iagoba Apellaniz. Quantum metrology from a quantum information science perspective. *Journal of Physics A: Mathematical and Theoretical*, 47(42), 2014.

All the codes in the different appendix sections have been uploaded to a *GitHub* repository for the reader's convenience. It can be found in the following link:

github.com/PauColomerSaus/Quantum-enhanced-estimation-of-a-mode-parameter.git

A Schwinger code

By inputting the number of photons and the constants c , d_1 and d_2 and selecting the number of photons, this code checks whether the quasi-optimal states obtained with the diagonalization method (section 3.1.3) and the Schwinger method (section 3.1.4) are equivalent. If they are, it outputs the quantum enhanced sensitivity that they achieve. It can be checked that this sensitivity coincides with the equation 32.

```

1 import qutip as q
2 import numpy as np
3
4 #Set the number of photons
5 N=15
6
7 #The dimension of the Schwinger-space
8 Nb=N/2
9
10 #set angle of radial displacement(if needed)
11 alpha=0
12
13 #set constants
14 cte=1.0j/np.sqrt(2)*np.exp(1j*alpha)
15 d1=2
16 d2=6
17
18 #Schwinger representation
19 #Generate H as a Jn
20 H=2*(q.operators.jmat(Nb,'x')*cte.real-
21       q.operators.jmat(Nb,'y')*cte.imag)
22
23 #An orthogonal direction to both Jz and Jn
24 Jm=2*(q.operators.jmat(Nb,'x')*np.cos(alpha)-
25       q.operators.jmat(Nb,'y')*np.sin(alpha))
26
27 #A rotation around Jm brings Jz to Jn
28 angle=np.pi/2
29 R=-1j*angle/2*Jm
30 U=R.expm()
31
32 #This has to be equal to H
33 test=np.sqrt(2)*(U.dag()*q.operators.jmat(Nb,'z')*U)
34
35 #The quasi-optimal state is
36 optz=1/np.sqrt(2)*(q.basis(N+1,0)+1j*q.basis(N+1,N))
37 opt=U*optz

```

```

38
39 #Diagonalization procedure
40 #Generate the Hamiltonian
41 H=0*q.num(N+1)
42 for k in range(N):
43     h=(np.sqrt((k+1)*(N-k))*(cte*q.basis(N+1,k+1)*q.basis(N+1,k).dag()+
44         np.conj(cte)*q.basis(N+1,k)*q.basis(N+1,k+1).dag()))
45     H=H+h
46
47 #This are the linear terms
48 Nd=d2*q.num(N+1)
49 for k in range(N):
50     Nd1=d1*(N-k)*q.basis(N+1,k)*q.basis(N+1,k).dag()
51     Nd=Nd1+Nd
52
53 #The quasi-optimal state is
54 opth=((H.eigenstates()[1])[0]+(H.eigenstates()[1])[N]).unit()
55
56 #The quasi-optimal sensitivities for the two procedures are
57 Fschw=4*q.expect(H**2,opt)-4*q.expect(H,opt)**2+q.expect(Nd,opt)
58 Fdiag=4*q.expect(H**2,opth)-4*q.expect(H,opth)**2+q.expect(Nd,opth)
59
60 Fcheckschw=np.round(Fschw,10)
61 Fcheckdiag=np.round(Fdiag,10)
62
63 if Fcheckschw==Fcheckdiag:
64     print('The two procedures get us equivalent quasi-optimal states')
65     print('The achieved sensitivity is:',Fcheckdiag)
66 else:
67     print('We do not get the equivalent states')

```


B Optimal state code

By inputting the constants c , d_1 and d_2 , and selecting a number of photons, this code checks whether the condition $\langle H_I \rangle_\psi = 0$ is fulfilled. If it is fulfilled it outputs the maximal sensitivity that can be obtained with the inputted system, the optimal state that achieves it, and the elements of an optimal measurement in the number of photons basis.

```
1 import qutip as q
2 import numpy as np
3
4 N=5
5 Nb=N/2
6 alpha=0
7 cte=1.0j/np.sqrt(2)*np.exp(1j*alpha)
8 d1=2
9 d2=6
10
11 #Generate the Hamiltonian with Schwinger
12 H=2*(q.operators.jmat(Nb,'x')*cte.real-
13       q.operators.jmat(Nb,'y')*cte.imag)
14 Jm=2*(q.operators.jmat(Nb,'x')*np.cos(alpha)-
15       q.operators.jmat(Nb,'y')*np.sin(alpha))
16 angle=np.pi/2
17 R=-1j*angle/2*Jm
18 U=R.expm()
19 H=np.sqrt(2)*(U.dag()*q.operators.jmat(Nb,'z')*U)
20
21 #This is the linear part
22 Nd=d2*q.num(N+1)
23 for k in range(N):
24     Nd1=d1*(N-k)*q.basis(N+1,k)*q.basis(N+1,k).dag()
25     Nd=Nd1+Nd
26
27 #The sensitivity is
28 S=4*H**2+Nd
29
30 #The eigenvector corresponding to the maximum eigenvalue is
31 opt=(S.eigenstates()[1])[N]
32 Fopt=4*q.expect(H**2,opt)-4*q.expect(H,opt)**2+q.expect(Nd,opt)
33 test=np.round(q.expect(H,opt),10)
34
35 if test==0:
36     print("The optimal sensitivity is:",Fopt)
37     print('The optimal state is:',opt )
38 else:
39     print('This procedure is not optimal')
40
41 #The symmetric logarithmic derivative
42 rho=opt*opt.dag()
43 L=2j*q.commutator(rho,H)
```

```
44
45 #The POVM elements
46 POVM=[]
47 idcheck=0
48 for k in range(N+1):
49     E= ((L.eigenstates()[1])[k])*((L.eigenstates()[1])[k]).dag()
50     POVM.append(E)
51
52     #Check it is a POVM
53     idcheck=idcheck+E
54     if idcheck == q.identity(N+1):
55         print("An optimal POVM is:")
56
57 print(POVM)
```

C Comparison code

This code outputs two plots. The first one is the plot of the quasi-optimal and the optimal sensitivities for different number of photons, the two lines are so close that it is important to set a small range for the plot (lines 49 to 52). The second is the difference between the optimal and the quasi-optimal sensitivities. The values of the constants c , d_1 and d_2 are in this code set for the radial displacement estimation case. They can be changed to obtain similar plots for the x and y -axis displacements with HG modes.

```
1 import qutip as q
2 import numpy as np
3 import matplotlib.pyplot as plt
4
5 alpha=0
6 cte=1.0j/np.sqrt(2)*np.exp(1j*alpha)
7 d1=2
8 d2=6
9
10 x=np.linspace(2,20,19)
11
12 dataan=[]
13 datamax=[]
14
15 #Evaluate the sensitivity for different numbers of photons
16 for N in range(2,21):
17
18     #This creates our hamiltonian
19     H=0*q.num(N+1)
20     for k in range(N):
21         h=(np.sqrt((k+1)*(N-k))*(cte*q.basis(N+1,k+1)*q.basis(N+1,k).dag()+
22             np.conj(cte)*q.basis(N+1,k)*q.basis(N+1,k+1).dag()))
23         H=H+h
24     san=((H.eigenstates()[1])[0]+(H.eigenstates()[1])[N]).unit()
25
26     #This adds the linear terms
27     Nd=d2*q.num(N+1)
28     for k in range(N):
29         Nd1=d1*(N-k)*q.basis(N+1,k)*q.basis(N+1,k).dag()
30         Nd=Nd1+Nd
31
32     #The quasi-optimal sensitivity
33     Fan=4*q.expect(H**2,san)-4*q.expect(H,san)**2+q.expect(Nd,san)
34     dataan.append(Fan)
35
36     #The optimal sensitivity
37     S=4*H**2+Nd
38     smax=(S.eigenstates()[1])[N]
39     Fmax=4*q.expect(H**2,smax)-4*q.expect(H,smax)**2+q.expect(Nd,smax)
40     datamax.append(Fmax)
41
```

```

42 #Plot both sensitivities
43 plt.plot(x,datamax,label='optimal sensitivity',linestyle='--')
44 plt.plot(x,dataan,label='Quasi-optimal sensitivity',linestyle='--')
45 plt.plot(x,datamax,'ro',color='blue',markersize=5)
46 plt.plot(x,dataan,'ro',color='orange',markersize=5)
47 plt.ylabel('Sensitivity')
48 plt.xlabel('Number of photons')
49 #Set a range so that the difference is visible
50 plt.xlim(2,5.1)
51 plt.xticks(np.arange(2,6,step=1))
52 plt.ylim(15,75)
53 plt.legend()
54 plt.show()
55
56 #Plot the difference
57 y=np.subtract(datamax,dataan)
58 plt.plot(x,y,'ro',color='blue', markersize=5)
59 plt.plot(x,y)
60 plt.xlim(2,20.1)
61 plt.ylim(0.4,1.8)
62 plt.xticks(np.arange(2,21,step=2))
63 plt.xlabel("Number of photons")
64 plt.ylabel("Sensitivity difference")
65 plt.show()

```

The plots we obtain by changing the constants $c = i$, $d_1 = 0$, and $d_2 = 8$ so that they match the x and y -axis displacements with two Hermite-Gauss modes are:

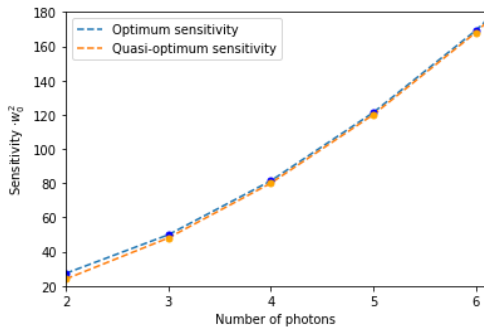


Figure 11: Comparison of the optimal and quasi-optimal sensitivities as a function of N

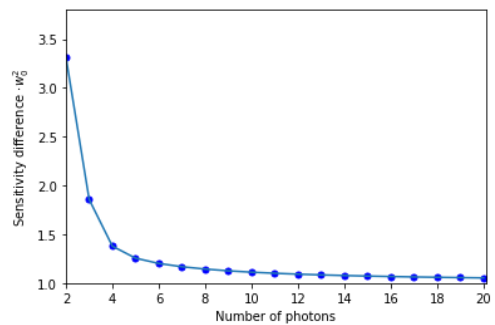


Figure 12: Difference between the optimal and quasi-optimal sensitivities as a function of N

D NOONs code

This code plots the populations of the primary, secondary, tertiary, quaternary and quinary NOONs as a function of the number of photons. Use lines 76 to 78 to zoom in a part of the plot and appreciate more clearly the function's behaviour.

```
1 import qutip as q
2 import numpy as np
3 import matplotlib.pyplot as plt
4
5 alpha=0
6 cte=1.0j/np.sqrt(2)*np.exp(1j*alpha)
7 d1=2
8 d2=6
9 x=np.linspace(2,10,9)
10 x3=np.linspace(4,10,7)
11 x4=np.linspace(6,10,5)
12 x5=np.linspace(8,10,3)
13 datanoon=[]
14 N2=[]
15 N3=[]
16 N4=[]
17 N5=[]
18
19 for N in range(2,11):
20
21     Nb=N/2
22
23     #This generates our Hamiltonian
24     H=0*q.num(N+1)
25     for k in range(N):
26         h=(np.sqrt((k+1)*(N-k))*(cte*q.basis(N+1,k+1)*q.basis(N+1,k).dag()+
27             np.conj(cte)*q.basis(N+1,k)*q.basis(N+1,k+1).dag()))
28         H=H+h
29
30     #This adds the d1 d2 terms
31     Nd=d2*q.num(N+1)
32     for k in range(N):
33         Nd1=d1*(N-k)*q.basis(N+1,k)*q.basis(N+1,k).dag()
34         Nd=Nd1+Nd
35
36     #The optimal state in Jn
37     S=4*H**2+Nd
38     smax=(S.eigenstates()[1])[N]
39     Fmax=4*q.expect(H**2,smax)-4*q.expect(H,smax)**2+q.expect(Nd,smax)
40
41     #An orthogonal direction to both Jz and Jn
42     Jm=2*(q.operators.jmat(Nb,'x')*np.cos(alpha)-
43         q.operators.jmat(Nb,'y')*np.sin(alpha))
44
```

```

45     #A rotation around Jm brings Jz to Jn
46     angle=np.pi/2
47     R=-1j*angle/2*Jm
48     U=R.expm()
49
50     #optimalstate in z direction
51     optH=U.dag()*smax
52
53     datanoon.append((np.sqrt(2)*np.absolute(optH[0])[0][0])**2)
54     N2.append((np.sqrt(2)*np.absolute(optH[1])[0][0])**2)
55     #Terciary NOON appears for N>=4
56     if N>3:
57         N3.append((np.sqrt(2)*np.absolute(optH[2])[0][0])**2)
58     #Quaternary NOON appears for N>=6
59     if N>5:
60         N4.append((np.sqrt(2)*np.absolute(optH[3])[0][0])**2)
61     #Quinary NOON appears for N>=8
62     if N>7:
63         N5.append((np.sqrt(2)*np.absolute(optH[4])[0][0])**2)
64
65     #Plot all NOONs
66     plt.plot(x,datanoon,linestyle='--',label='NOON state')
67     plt.plot(x,datanoon,'ro',color='blue',markersize=5,)
68     plt.plot(x,N2,linestyle='--',label='Secondary NOON')
69     plt.plot(x,N2,'ro',color='orange',markersize=5)
70     plt.plot(x3,N3,linestyle='--',label='Tertiary NOON')
71     plt.plot(x3,N3,'ro',color='green',markersize=5,)
72     plt.plot(x4,N4,linestyle='--',label='Quaternary NOON')
73     plt.plot(x4,N4,'ro',color='red',markersize=5,)
74     plt.plot(x5,N5,linestyle='--',label='Quinary NOON')
75     plt.plot(x5,N5,'ro',color='purple',markersize=5,)
76     #Set axis limits if you want to zoom in
77     #plt.xlim(4,8.1)
78     #plt.ylim(0,0.03)
79     plt.legend()
80     plt.xlabel('Number of photons')
81     plt.ylabel('Population')
82     plt.show()

```

This code is far from efficient but has been redacted this way in order to be more readable.

The figures 6 and 7 in the text are plotted with the constants corresponding to the estimation of a radial displacement with LG modes. We could add here the equivalent plots for the x and y -axis displacements with LG modes like we did in appendix C. But there is no visible difference between them, so they are omitted.

E Sensitivities for different angles

This code plots the sensitivities on the estimation of a radial displacement populating HG or LG codes as a function of the displacement angle. Notice that the shape of the plot is the same $\forall N$, the only thing that changes is the range of the sensitivity.

```
1 import qutip as q
2 import numpy as np
3 import matplotlib.pyplot as plt
4
5 dataHG=[]
6 dataLG=[]
7 dataHGy=[]
8
9 x=np.linspace(2,15,13)
10 angles=np.linspace(0,2*np.pi,400)
11 theta = np.arange(0, 2*np.pi+np.pi/4, step=(np.pi/4))
12
13 N=2
14
15
16
17 for alpha in angles:
18     cte=[1j*np.cos(alpha),1j*np.sin(alpha),1j/np.sqrt(2)*np.exp(1j*alpha)]
19     d1=[4*np.sin(alpha)**2, 4*np.cos(alpha)**2, 2]
20     d2=[4*(1+np.cos(alpha)**2), 4*(1+np.sin(alpha)**2) , 6]
21
22     for g in range(3):
23
24         #This creates our hamiltonian
25         H=0*q.num(N+1)
26         for k in range(N):
27             h=(np.sqrt((k+1)*(N-k))*(cte[g]*q.basis(N+1,k+1)*q.basis(N+1,k).dag()+
28                 np.conj(cte[g])*q.basis(N+1,k)*q.basis(N+1,k+1).dag()))
29             H=H+h
30
31         #This adds the d1 d2 terms
32         Nd=d2[g]*q.num(N+1)
33         for k in range(N):
34             Nd1=d1[g]*(N-k)*q.basis(N+1,k)*q.basis(N+1,k).dag()
35             Nd=Nd1+Nd
36
37         #The best one is the maximum eigenvalue of the operator:
38         S=4*H**2+Nd
39         lmax=(S.eigenstates()[0])[N]
40         smax=(S.eigenstates()[1])[N]
41         Fmax=4*q.expect(H**2,smax)-4*q.expect(H,smax)**2+q.expect(Nd,smax)
42
43     if g==0:
44         dataHG.append(Fmax)
```

```

45     if g==1:
46         dataHGy.append(Fmax)
47     if g==2:
48         dataLG.append(Fmax)
49
50     #plot figure
51     plt.plot(angles,dataHG,label='$HG_{00}$ and $HG_{10}$')
52     plt.plot(angles,dataHGy,label='$HG_{00}$ and $HG_{01}$')
53     plt.plot(angles,dataLG,label='$LG_{0}^0$ and $LG_{0}^1$')
54     plt.xticks(theta, ['0', '\u03C0/4', '\u03C0/2', '3\u03C0/4',
55         '\u03C0', '5\u03C0/4', '3\u03C0/2', '7\u03C0/4', '2\u03C0'])
56     plt.margins(x=0)
57     plt.legend()
58     plt.xlabel('Displacement angle')
59     plt.ylabel('Sensitivity $\cdot w_0^2$')
60     plt.show()
61
62     #calculate the average
63     avLG=np.round(np.average(dataLG))
64     avHG=np.round(np.average(dataHG))
65     avHGy=np.round(np.average(dataHGy))
66
67     #compare the averages
68     if avLG>avHG:
69         print('Laguerre modes give a ',(avLG-avHG)*100/(avLG),
70             '% better sensitivity on average')
71     if avLG==avHG:
72         print('Laguerre and Hermite modes give the same sensitivity on average')
73     if avLG<avHG:
74         print('Hermite modes give a ',(-avLG+avHG)*100/(avLG) ,
75             '% better sensitivity on average')

```


F Actual mode shape of the four strategies in figure 8

We plot in this annex the shape of the modes we superpose with four different strategies in figure 8 in section 3.1.6. We also provide the codes used to plot the figures.

a) *Shapes of the HG modes:*

Shapes of the HG modes:

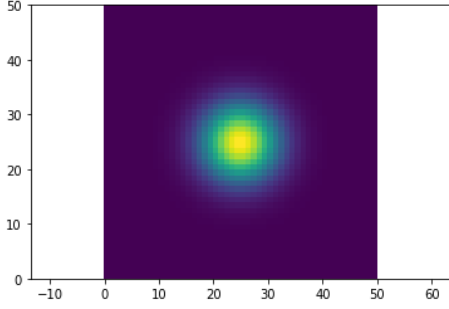


Figure 13: Intensity-shape of the HG_{00} mode

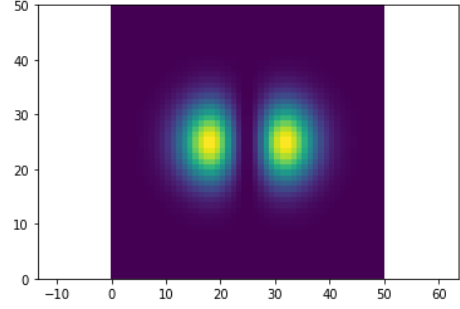


Figure 14: Intensity-shape of the HG_{10} mode

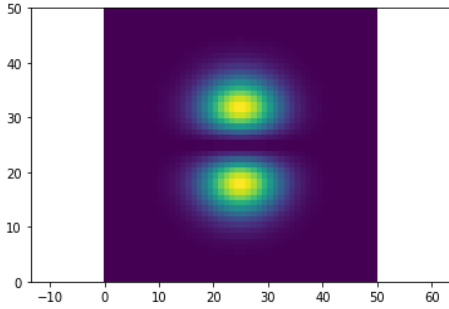


Figure 15: Intensity-shape of the HG_{01} mode

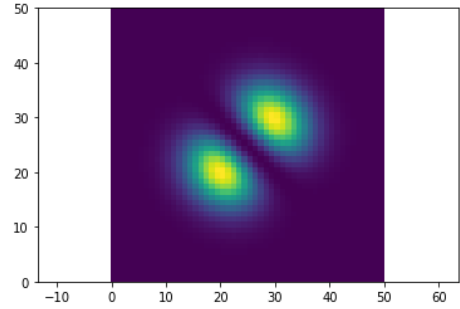


Figure 16: $\cos \alpha HG_{10} + \sin \alpha HG_{01}$ mode

This figures can be obtained with the following code. We can see how the excited modes have exactly the same shape but with rotated axis.

```

1 import numpy as np
2 import matplotlib.pyplot as plt
3
4 #set maximum indices
5 n = 0
6 m = 0
7 w0 = 2.0 # Arbitrary waist
8 k = 2*np.pi/532.0e-9 # Arbitrary wavenumber of light
9 alpha=np.pi/4
10 zR = k*w0**2.0/2; # Calculate the Rayleigh range
11
12 # Setup the cartesian grid for the plot at plane z
13 z = 0.0;
14 [xx, yy] = np.meshgrid(np.linspace(-5, 5), np.linspace(-5, 5))
15
16 def hermiteH(n, x):

```

```

17     if n == 0:
18         return 1;
19     elif n == 1:
20         return 2*x;
21     else:
22         return 2*x*hermiteH(n-1, x) - 2*(n - 1)*hermiteH(n - 2, x)
23
24 U00 = 1.0/(1 + 1j*z/zR)*np.exp(-(xx**2 + yy**2)/w0**2/(1 + 1j*z/zR))
25 Hn = hermiteH(n, xx)
26 Hm = hermiteH(m, yy)
27 Hm1= hermiteH(m+1, yy)
28 Hn1= hermiteH(n+1, xx)
29
30 U = U00*Hn*Hm*np.exp(-1j*(n + m)*np.arctan(z/zR))    #for HG00
31 V = U00*Hn*Hm1*np.exp(-1j*(n + m+1)*np.arctan(z/zR)) #for HG01
32 W = U00*Hn1*Hm*np.exp(-1j*(n+1 + m)*np.arctan(z/zR)) #for HG10
33 X = np.cos(alpha)*V+np.sin(alpha)*W                  #for sin(a)HG10+cos(a)HG01
34
35 plt.figure()
36 plt.pcolor(abs(X)**2); #Change for V, W or X to see the corresponding plots
37 plt.axis('equal')
38
39 plt.show()

```

a) Shapes of the LG modes:

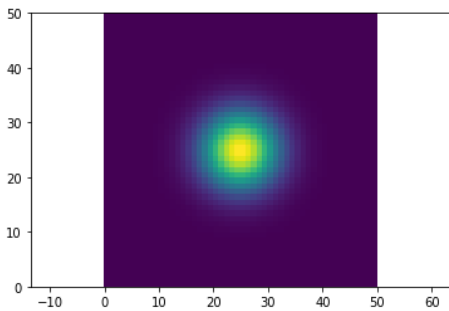


Figure 17: Intensity-shape of the LG_0^0 mode

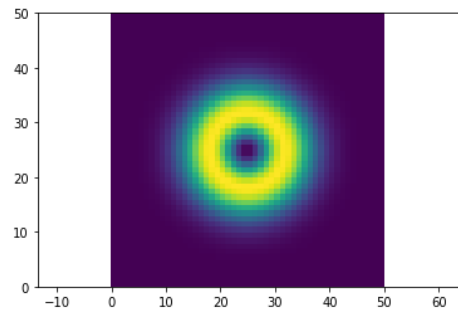


Figure 18: Intensity-shape of the LG_0^1 mode

This figures can be obtained with the similar code:

```

1 import numpy as np
2 import matplotlib.pyplot as plt
3 import scipy
4
5 p = 0          # Degree of LG mode
6 l = 1         # Order of LG mode
7 w0 = 2.0      # Beam waist
8 k = 2*np.pi/532.0e-9 # Wavenumber of light
9
10 zR = k*w0**2.0/2 # Calculate the Rayleigh range

```

```

11
12 # Setup the cartesian grid for the plot at plane z
13 z = 0.0
14 xx, yy = np.meshgrid(np.linspace(-5, 5), np.linspace(-5, 5))
15
16 # Calculate the cylindrical coordinates
17 r = np.sqrt(xx**2 + yy**2)
18 phi = np.arctan2(yy, xx)
19
20 U00 = 1.0/(1 + 1j*z/zR) * np.exp(-r**2.0/w0**2/(1 + 1j*z/zR))
21 w = w0 * np.sqrt(1.0 + z**2/zR**2)
22 R = np.sqrt(2.0)*r/w
23
24 Lp1 = scipy.special.comb(p+1,p) * np.ones(np.shape(R))
25 for m in range(1, p+1):
26     Lp1 = (Lp1 + (-1.0)**m/scipy.special.factorial(m) *
27           scipy.special.comb(p+1,p-m) * R**(2.0*m))
28
29 U = U00*R**1*Lp1*np.exp(1j*1*phi)*np.exp(-1j*(2*p + 1 + 1)*np.arctan(z/zR))
30
31 plt.figure()
32 plt.pcolor(abs(U)**2)
33 plt.axis('equal')
34
35 plt.show()

```

G Random state generation

This code creates a 100.000 random states and calculates the sensitivity they achieve in the estimation of the wavelength when populating a single mode. The maximal of this random state sensitivities is compared with the sensitivity obtained with the quasi-optimum state. The code plots in orange the quasi-optimum sensitivities and in blue the maximal sensitivities obtained with random states for $N \in [2, 6]$.

```
1 import qutip as q
2 import numpy as np
3 import matplotlib.pyplot as plt
4
5 a=1
6 b=2
7
8 dataqF=[]
9 dataF=[]
10 x=np.linspace(2,6,5)
11
12 for N in range(2,7):
13     #Calculate the sensitivity with a random state
14     check=0
15     numoptstate=q.basis(N+1,0)
16     for k in range(100000):
17         state=q.rand_ket(N+1).unit()
18         F=a*q.variance(q.num(N+1),state)+b*q.expect(q.num(N+1),state)
19         if F>check:
20             check=F
21             numoptstate=state
22     dataF.append(F)
23
24     #the sensitivity with the NOON
25     NOON=(q.basis(N+1,0)+q.basis(N+1,N)).unit()
26     qF=a*q.variance(q.num(N+1),NOON)+b*q.expect(q.num(N+1),NOON)
27     dataqF.append(qF)
28
29 plt.plot(x,dataF,label='Best out of 100000 random',linestyle='--')
30 plt.plot(x,dataqF,label='Quasi-optimal sensitivity',linestyle='--')
31 plt.plot(x,dataF,'ro',markersize=5, color='blue')
32 plt.plot(x,dataqF,'ro',markersize=5, color='orange')
33 plt.legend()
34 plt.xlabel('Number of photons')
35 plt.ylabel('Normalized sensitivity')
36 plt.show()
```